Trop J Nat Prod Res, January 2026; 10(1):6844 – 6860
ISSN 2616-0684 (Print)
ISSN 2616-0692 (Electronic)

Tropical Journal of Natural Product Research

Available online at https://www.tjnpr.org

Original Research Article

Anticancer Activity of the Endophytic Fungus *Phomopsis* sp. Against MCF-7 Breast Cancer Cells: *In vitro* and *In silico* Studies

Maheswari A. Dwicesaria[1], Bambang P. Priosoeryanto[2], Akhmad E. Hasan[1], Riyan A. P. Irsal[3], Gusnia M. Gholam[1], Fachrur R. Mahendra[1], Syaefudin Suminto[1,4,5]*

[1]*Department of Biochemistry, Faculty of Mathematics and Natural Sciences, IPB University, Dramaga Campus, Bogor 16680, Indonesia*
[2]*School of Veterinary Medicine and Biomedicine, IPB University, Bogor 16800, Indonesia*
[3]*Applied Chemistry, Faculty of Engineering, Kyushu University, Nishi-ku, Fukuoka 819-0395, Japan*
[4]*Tropical Biopharmaca Research Center, IPB University, Bogor, 16128, Indonesia*
[5]*Bioinformatics Study Program, Faculty of Mathematics and Natural Sciences, IPB University, Bogor, 16680, Indonesia*

ARTICLE INFO

Article history:
Received 25 October 2025
Revised 13 January 2025
Accepted 16 January 2026
Published online 01 February 2026

ABSTRACT

Breast cancer is a major global health concern, increasing the demand for alternative therapeutic sources. Therefore, this study aims to evaluate the anticancer potential of the endophytic fungus *Phomopsis* sp. from soursop leaves against MCF-7 breast cancer cells. The metabolite profile of *Phomopsis* sp. was analyzed, and the anticancer as well as apoptotic activity were assessed in both MCF-7 and normal Vero cell lines. The samples were cultivated in yeast malt broth, extracted with ethyl acetate, and separated using column chromatography. The result showed that Brine shrimp lethality test yielded ten fractions (F1–F10), with F1 demonstrating the strongest cytotoxicity (LC_{50} = 2.33 µg/mL). Antiproliferative assays produced IC_{50} values of 5.65 µg/mL for MCF-7 and 5.21 µg/mL for Vero cells, with apoptosis confirmed by acridine orange-ethidium bromide staining. Furthermore, Liquid Chromatography-tandem Mass Spectrometry (LC-MS/MS) identified 38 active compounds in the F1 sample, including known anticancer agents such as cytosporone C, kynurenic acid, maraniol, (-)-caryophyllene oxide, and chalcone. Computational *in silico* analyses using PASS online, molecular docking, ADMET/pharmacokinetic studies, density functional theory (DFT) analysis, and molecular dynamics (MD) simulations further validated chalcone as a promising anticancer candidate. Chalcone showed favorable ADMET/pharmacokinetic properties and achieved the highest docking score of-8.392 kcal/mol among the compounds tested. MD simulations over 300 ns indicated that chalcone outperformed tamoxifen, with binding energy calculations showing a value of -227.069 kJ/mol compared to -45.598 kJ/mol for tamoxifen. In conclusion, these results underscore the therapeutic potential of endophytic fungi as sources of novel agents for breast cancer treatment.

Keywords: Apoptosis, Breast cancer, *Phomopsis* sp., Molecular dynamics, Quantum chemistry, Density Functional Theory

Introduction

Globally, cancer ranks as the second most common cause of death, responsible for about one out of every six deaths. The World Health Organization, through the Global Cancer Observatory (GLOBOCAN), reported that cancer led to nearly 9 million fatalities in 2022.[1] Breast cancer is the most prevalent among newly diagnosed cancers. GLOBOCAN data show that in 2020, breast cancer ranked first in incidence and fifth in cancer-related mortality, contributing to 11.5% of all new cancer cases diagnosed in 2022. From the total cancer-related deaths reported in 2022, 6.8% were attributable to breast cancer.[1]

*Corresponding author. E mail: syaefudin01@apps.ipb.ac.id
Tel: +62 813-1821-4267

Citation: Dwicesaria MA, Priosoeryanto BP, Hasan AZ, Irsal RAP, Gholam GM, Mahendra FR, Suminto S. Anticancer Activity of the Endophytic Fungus *Phomopsis* sp. Against MCF-7 Breast Cancer Cells: *In vitro* and *In silico* Studies. Trop J Nat Prod Res. 2026; 10(1): 6844 – 6860
https://doi.org/10.26538/tjnpr/v10i1.56

Official Journal of Natural Product Research Group, Faculty of Pharmacy, University of Benin, Benin City, Nigeria

A variety of therapeutic options are currently available for cancer patients, including radiotherapy, mastectomy, and chemotherapy. In metastatic cancer, chemotherapy is more effective than radiotherapy or mastectomy.[2] Despite the strong therapeutic impact, chemotherapy is associated with significant adverse effects because the drugs attack both cancer and normal cells. Normal somatic cells adversely affected are generally those with high proliferative activity, including hematopoietic cells in the bone marrow, hair follicle cells, and gastrointestinal epithelial cells.[3] Considering the severity of the side effects, it is necessary to develop another option for cancer treatment that can provide minimal side effects with high therapeutic efficacy.
Several studies have shown that endophytes are a promising source of anticancer drugs. The discovery of the billion-dollar chemotherapeutic drug paclitaxel, derived from *Taxus longifolia*, has significantly increased studies on endophytic anticancer activity.[4] More than 800 genera of endophytic fungi have been reported, with the most frequently isolated being *Phomopsis*, *Gibberella*, *Alternaria*, *Nigrospora*, *Guignardia*, *Fusarium*, *Glomerella*, *Leptosphaerulina*, *Phoma*, *Colletotrichum*, and *Xylaria*.[5] *Phomopsis* spp. and the teleomorph *Diaporthe* are most commonly found in tropical plants.[6,7] Although *Phomopsis* sp. can be found in many plants, including soursop, cocoa, coffee, mango, and red frangipani,[8,9] there are no detailed reports on the anticancer and apoptotic activity of samples collected from soursop leaves.

In a previous study, Minarni *et al.*,[10] found that an endophytic fungus from the leaves of the soursop plant (*Annona muricata* L.) identified as *Phomopsis* sp. showed good anticancer potential against the breast cancer cell line MCF-7 with an IC_{50} value of 19.20 ± 7.71 µg/mL. Other studies [11,12] also reported that soursop leaves inhibited the growth of colon (WiDr) and cervix (HeLa) cancer cell lines, with IC_{50} = 20.80 µg/mL and 11.71 µg/mL, respectively.

The main advantage of endophytic fungi is the easy extraction and stability of secondary metabolites. Endophytic fungi are easy to culture in different fermentation media, and consistently secrete metabolites which produce bioactive compounds, including paclitaxel, podophyllotoxin, vinca alkaloids, camptothecin, hypericin, emodin, azadirachtin, and deoxypodophyllotoxin, used therapeutically to target cancer and other diseases.[13–16] *Phomopsis* sp. secretes several bioactive compounds capable of increasing the antiproliferative activity against cancer cells, with the most common being polyketides, terpenoids, steroids, macrolides, alkaloids, and flavonoids.[17]

Aside from *in vitro* studies, computational *in silico* methods, such as molecular docking, molecular dynamics (MD) simulations, density functional theory (DFT), and Prediction of Activity Spectra for Substances (PASS) analysis, offer valuable insights into the interaction of bioactive compounds with specific molecular targets. These methods have been widely used to predict the binding affinity, stability, and potential activity of natural products, including endophytic fungal metabolites, against cancer targets. Molecular docking enables the prediction of ligand-receptor interactions at the atomic level, while MD simulations further analyze the stability of these interactions over time. DFT studies provide a deeper understanding of the electronic structure of molecules and offer insights into the reactivity and interaction potential. PASS analysis predicts the biological activity spectra of compounds, allowing for the identification of promising drug candidates.[18–20] Despite the potential, *in silico* studies on secondary metabolites from *Phomopsis* sp. derived from soursop leaves remain underexplored. Previous studies used *in vitro* assays but did not provide comprehensive *in silico* computational data. Therefore, this study aims to analyze the metabolite content of *Phomopsis* sp. along with the anticancer and apoptotic activity against human breast cancer (MCF-7) and normal (Vero) cell lines by integrating *in vitro* and computational *in silico* methods to complement experimental data.

Materials and Methods

The materials used in this study include isolates of *Phomopsis* derived from soursop leaves collected in Garut, Indonesia, located geographically at latitude –7.227906 and longitude 107.908699, yeast malt broth (YMB) (HiMedia, India), ethyl acetate, dimethyl sulfoxide (DMSO) (Merck, US), and silica gel 60 70-230 mesh (Merck, US). Other materials include methanol (BrataChem, Indonesia), hexane (BrataChem, Indonesia), 70% ethanol (BrataChem, Indonesia), fetal bovine serum (FBS) (Merck, US), fetal calf serum (FCS) (Merck, US), Dulbecco's Modified Eagle Medium (DMEM) (Sigma Aldrich, US), phosphate-buffered saline (PBS) (Sigma Aldrich, US), MCF-7 cells, Vero cells, thin-layer chromatography (TLC) plates 60 F254 (Merck, US), ethidium bromide (EB) (Sigma Aldrich, US), acridine orange (AO) (Sigma Aldrich, US), and tamoxifen (TAM) (Merck, US). Meanwhile, the instruments used were a rotary evaporator (LabTech, Italy), Olympus CX-23 light microscope (Olympus, Japan), ZEISS LSM 980 Confocal Laser Scanning Microscope (Zeiss, Germany), and LC-MS/MS UHPLC Vanquish Tandem Q Exactive Plus Orbitrap HRMS ThermoScientific (ThermoScientific, US). *In silico* computational analysis was conducted using estrogen receptor alpha (ERα) with PDB ID: 2IOG (rcsb.org/structure/2IOG). The molecular structures of the candidate compounds and tamoxifen were obtained from PubChem (pubchem.ncbi.nlm.nih.gov/). The software used include YASARA (version 19.9.17), Gaussian 09W and GaussView (version 5.0), Discovery Studio (version 2024), GraphPad Prism (version 8, San Diego, CA, USA), R-Studio (R 3.6.0+, from Posit), and Visual Molecular Dynamics (VMD) (Theoretical and Computational Biophysics Group, University of Illinois at Urbana-Champaign).

In vitro assays

Extraction of Phomopsis sp.

Phomopsis sp. was inoculated into industrial-scale production, and 500 L of YMB was used in a bioreactor to obtain bioactive compounds. The extract was concentrated using a rotary vacuum evaporator.

Optimization of eluent with TLC

Chromatography was performed on an activated 3 × 6 cm TLC plate sterilized using methanol, followed by incubation in an oven at 105 °C for 1 min. Lines were drawn 1 cm from the top and bottom edges of the plate. The endophytic fungal extract was dissolved in methanol and spotted onto a TLC plate using thin capillary pipettes. After the spot was dried, the plate was eluted in a chromatographic chamber filled with 10 mL of saturated eluent (mobile phase) for 10 min.

The samples were eluted with 100% hexane, 100% ethyl acetate, 100% methanol, or a combination of both, and the plate was removed after the eluent reached the top edge. The plates were air-dried, and the elution stains were observed under UV light at wavelengths of 254 and 366 nm. The eluent that showed the highest staining and good separation was selected.

Separation with column chromatography

The ethyl acetate extract of *Phomopsis* sp. was purified using silica gel 60 (0.063–0.200 mm) for column chromatography (70–230 mesh ASTM; Merck, New Jersey, USA) as the stationary phase with a dry packing column. A solvent gradient system with ethyl acetate, methanol, and hexane was used as the mobile phase eluent, with increasing polarity in the following combinations: hexane:ethyl acetate (9:1 v/v), hexane:ethyl acetate (7:3 v/v), hexane:ethyl acetate (5:5 v/v), methanol:ethyl acetate (5:5 v/v), and methanol:ethyl acetate (10:0 v/v).

Brine shrimp lethality assay

Fractions were prepared through column chromatography for the Brine Shrimp Lethality Test (BSLT) by dissolving 15 mg of each sample in 20 mL of seawater supplemented with 1% DMSO to form stock solutions. Subsequent dilutions were made to achieve a final concentration of 1500 µg/mL, which was further diluted to 1000, 100, and 10 µg/mL. Brine shrimp were hatched in a controlled chamber filled with seawater at room temperature, using a light source provided for a duration of 48 h. Following the hatching period, ten brine shrimp were transferred to each well of a 12-well microplate, and the total volume in each well was adjusted with seawater to attain the desired final concentrations. Each concentration was tested in triplicate, and after a 24 h exposure period, probit analysis was used to determine the LC_{50} value, which represents the lethal concentration of a substance that induces 50% mortality in the sample population.[21]

Antiproliferation activity with trypan blue assay

The sample with the lowest LC_{50} value for the antiproliferation assay using tamoxifen (TAM) was selected as a positive control. Subsequently, the trypan blue exclusion assay was conducted on both MCF-7 and Vero cell lines following the methodology established by Alanuqaydan *et al.*[22] *Phomopsis* sp. samples were prepared by dissolving 32, 16, 8, 4, 2, and 1 µg/mL in DMEM supplemented with 1% DMSO. The cell suspensions were seeded into 24-well culture plates, treated accordingly, and incubated for 72 h. Live cell counts were determined using a hemocytometer (Marienfeld, Germany). The percentage of viable cells at each concentration was then calculated as the ratio of the number of live cells in the sample to that in the control group. Linear regression analysis was further performed on the data collected over the 72-h period, enabling the calculation of the IC_{50} values for each concentration according to equations (Eq.) 1 and 2:

$$\text{Percentage viability} = \left(\frac{\text{Number of treated live cells counted}}{\text{Number of control live cells counted}}\right) \times 100\% \quad \text{Eq. (1)}$$

$$\text{Percentage inhibition} = 100\% - \text{percentage viability} \quad \text{Eq. (2)}$$

Apoptosis assay

The apoptotic mechanism of the endophytic fungus extracted from soursop leaves was investigated following a protocol adapted from Setiawati [23] with slight modifications. MCF-7 cells were seeded onto a coverslip in a Petri dish and incubated for 24 h at 37 °C in a 5% CO_2 incubator. Subsequently, the culture medium was rinsed with PBS. The well plate was filled with 5 µg/mL of the sample in DMEM (Sigma-Aldrich, St. Louis, MO, USA) and incubated for 72 h. After incubation, the MCF-7 cells were washed with PBS to eliminate the residual medium. The coverslips were carefully removed and transferred onto glass slides. Subsequently, the slides were immersed in a mixture of acridine orange and ethidium bromide (AO–EB) and examined using a ZEISS LSM 980 confocal laser-scanning fluorescence microscope.

Compounds identification with LC–MS/MS

Liquid chromatography–tandem mass spectrometry (LC–MS/MS) analyses were conducted using a UHPLC Vanquish Tandem Q Exactive Plus Orbitrap High-Resolution Mass Spectrometer (Thermo Fisher Scientific, Massachusetts, USA) equipped with an Accucore C_{18} column (100 × 2.1 mm, 1.5 µm). An injection volume of 2.0 µL was used, and the mass range was set from 200 to 1500 m/z. Solvent A consisted of 0.1% formic acid (FA) in deionized water, and solvent B comprised 0.1% FA in acetonitrile. The total flow rate was maintained at 0.200 mL/min. The isocratic elution program comprised the following steps: 0–1.0 min (5% B), 1–25 min (5–95% B), 25–28 min (95% B), and 28–35 min (5% B). Chromatograms were constructed using the Compound Discoverer software.

Computational studies

Protein preparation

The ERα protein with PDB ID: 2IOG (rcsb.org/structure/2IOG) was used in the computational studies. After being downloaded, the protein was prepared using the YASARA Structure software for molecular docking. The preparation comprised the removal of water molecules and the co-crystallized ligand N-[(1R)-3-(4-hydroxyphenyl)-1-methylpropyl]-2-[2-phenyl-6-(2-piperidin-1-ylethoxy)-1H-indol-3-yl]acetamide. Hydrogen atoms were also added during this process, and the Erα protein was then stored in (*.pdb) format. [24]

Ligand structural preparation

The structures of the test compounds (ligands) from the LC-MS/MS F1 analysis of the soursop leaf endophytic fungus, along with the control drug tamoxifen, were retrieved from PubChem (pubchem.ncbi.nlm.nih.gov). The ligands were prepared for molecular docking using the YASARA Structure by adding hydrogen atoms, adjusting pH to optimize bond configurations and hydrogen interactions, as well as applying the NOVA force field and then energy minimization. Each ligand structure was saved in (*.pdb) format, and all the structures were subsequently combined and saved in (*.ligands.sdf, respectively). [25]

PASS analysis

Prediction of the activity spectra for substances (PASS) for each ligand was performed using the PASS online tool (way2drug.com/passonline/index.php). This process started with the retrieval of Canonical SMILES data for each ligand from the PubChem database. Subsequently, these SMILES were uploaded to the PASS online server, which facilitated the prediction of the biological activity spectra for each ligand based on the provided data. The systematic approach enabled a comprehensive assessment of the potential biological activity of the ligands. [25]

Molecular Docking

The test compounds were docked as potential drug candidates against the ERα protein (PDB ID: 2IOG) using YASARA software. The docking simulations used the VINA algorithm in conjunction with AMBER14, resulting in 100 runs managed through a macro file named `dock_runscreening.' The bounding box for these simulations was set with dimensions of X-size (65.81 Å), Y-size (65.81 Å), and Z-size (65.81 Å), forming a cube with a measurement of 5 Å. In this setup, Erα was maintained in a rigid conformation, while the test compounds were treated as flexible entities. This approach enabled a detailed analysis of the interactions between the test compounds and Erα protein, providing insights into the potential as drug candidates.[26]

ADMET/Pharmacokinetics studies

The compounds identified as potential drug candidates for breast cancer were analyzed for absorption, distribution, metabolism, excretion, toxicity (ADMET), and pharmacokinetic properties. This assessment used two widely recognized web servers, namely SwissADME (swissadme.ch) and pkCSM (biosig.lab.uq.edu.au/deeppk/). By extracting and analyzing the data obtained from the platforms, this study intends to identify drug candidates safe for humans. [27,28]

DFT analysis

The selected compounds were subjected to geometric optimization using DFT with the B3YLP functional and 6-31G (D,P) basis set. The calculations were performed using Gaussian 09 W and analyzed using the GaussView software (version 5.0). The energies of the lowest unoccupied molecular orbital (LUMO), highest occupied molecular orbital (HOMO), and energy gap were compiled. Based on these energy values, the global chemical reactivity descriptors were calculated and evaluated, including the ionization potential (I), electron affinity (A), chemical potential (µ), electronegativity (χ), hardness (η), softness (S), and electrophilicity index (ω) [29]. The energy gap was calculated using Eq. (3):

$E_{HOMO} - E_{LUMO}$ (Eq. 3)

The ionization potential (I) and electron affinity (A) were calculated using Equations (4) and (5), respectively.

$I = -E_{HOMO}$ (Eq. 4)
$A = -E_{LUMO}$ (Eq. 5)

The global chemical reactivity descriptors were calculated as follows:

Chemical potentials (µ) $= -\frac{(I + A)}{2}$ (Eq. 6)

Electronegativity (χ) $= \frac{(I + A)}{2}$ (Eq. 7)

Softness (S) $= \frac{1}{2\eta}$ (Eq. 8)

Hardness (η) $= \frac{(I - A)}{2}$ (Eq. 9)

Electrophilicity index (ω) $= \frac{\mu^2}{2\eta}$ (Eq. 10)

MD simulation

This study implemented several parameters during the pre-simulation phase for the selected protein-ligand complex and the control drug-protein complex. In the macro file `md_run.mcr`, the following algorithm settings were established: pH 7.4, 0.9% NaCl (physiological solution), 310 K, water density of 0.997 g/ml, MD simulation trajectory of 300 ns, and the AMBER14 force field. The MD simulation data were saved in the "sim" format. For post-MD analysis, the algorithm in the macro file `md_analyze` was used to obtain quantitative data for the root mean square deviation (RMSD), radius of gyration (Rg), solvent-accessible surface area (SASA), and hydrogen bonds. Additionally, the macro file `md_analyzeres,' which contains the algorithm for calculating the root mean square fluctuation (RMSF), was also used[26]

Calculation of binding energy using MM-PBSA

Binding energy calculations for the selected protein-ligand complex and the control drug-protein complex were performed using the Molecular Mechanics Poisson–Boltzmann Surface Area (MM-PBSA) method. YASARA provided an algorithm to obtain quantitative binding energy data, located in the macro file `md_bindenergy.mcr`.[30] The MM-PBSA calculations used the following equation:

ISSN 2616-0684 (Print)
ISSN 2616-0692 (Electronic)

Binding Energy = $E_{potRecept}$+ $E_{solvRecept}$+$E_{potLigand}$+$E_{solvLigand}$-$E_{potComplex}$-$E_{solvComplex}$ (Eq. 11)

PCA and Dynamic Cross-Correlation Matrix (DCCM)

Initially, the format of the protein-ligand complex obtained from the MD simulation trajectory was converted. YASARA provided the trajectory in "sim" format, which was transformed into "xtc" format using the macro file `md_convert.' Subsequently, this file was processed using the VMD software to generate a "dcd" file. The "pdb" and "dcd" formats for the selected complex were combined into a single working folder corresponding to each protein-ligand complex. Principal Component Analysis (PCA) was used to analyze the post-MD data for the selected protein-ligand complex through R Studio. To conduct this analysis, the function "mktrj.pca" from the Bio3D package was used to analyze the 300 ns trajectory data of the selected protein-ligand complex. The atomic movements within the protein and the relationship with stability was analayzed by performing PCA on the fluctuations in the Cα atoms. This process started with the removal of solvents and ions, followed by the calculation of eigenvalues and eigenvectors from the top three principal components (PCs). The values reflect the vectors in the matrix, which can predict and describe the primary directions of atomic movement. For the DCCM analysis, R Studio and the "dccm()" function were used from the Bio3D package. This function facilitated the calculation and analysis of the DCCM for the selected protein-ligand complex over the 300 ns MD trajectory [31].

Results and Discussion

In vitro analysis

Measuring cytotoxicity activity with the BSLT

A BSLT evaluates the cytotoxicity of a solution by using probit analysis to calculate the lethal concentration (LC_{50}). [32] Based on the metabolic similarity of *Artemia salina* to mammalian systems, which results in a similar toxicity response, BSLT appear to be the most reliable cytotoxicity activity assay for this study.[33]. Brine shrimp (*Artemia salina*) larvae used in this assay were 48 hours old and at the instar I–III developmental stages, characterized by fully developed limbs and high sensitivity to test substances [34]. Specifically, the BSLT estimates a sample lethal concentration as the LC_{50}. According to Meyer *et al.*, [35] natural compounds with LC_{50} < 1000 µg/mL are highly toxic, and cytotoxic compounds have been identified as highly potent anticancer agents.[36]

BSLT was used to examine the cytotoxicity of the extracts and fractions. Based on the probit analysis results, the *Phomopsis* sp. extract and fractions showed high cytotoxicity overall, as presented in Table 1. For eight of the ten samples, the LC_{50} was less than 1000 µg/mL. Natural compounds with LC_{50} < 1000 µg/mL are toxic and have potential anticancer activity.[35] The most toxic compound was fraction 1 (F1), with an LC_{50} of 2.33 µg/mL, followed by the extract (E) (LC_{50} = 6.88 µg/mL), and fraction 6 (F6) (LC_{50} = 40.10 µg/mL). Extracts and Fractions 1 (F1) to 8 (F8) had LC_{50} < 1000 µg/mL, showing significant potential as anticancer agents. This result was also lower than Handayani *et al.* [37] BSLT report of LC_{50} at 23.3 µg/mL for an ethyl acetate extract of *Phomopsis* sp. derived from marine sponges. The toxicity observed in the *Phomopsis* sp. fraction is possibly derived from the bioactive metabolites. According to Xu et al., [38] the cytotoxic activity of *Phomopsis*-derived extracts is commonly associated with metabolites belonging to the xanthone, chromone, chromanone, benzofuran, pyrone, quinone, phenolic, and oblongolide classes. Aside from the cytotoxic properties, these compounds are also known to possess diverse biological activity, including antifungal, anti-inflammatory, antibacterial, and other pharmacologically relevant effects.

Table 1: Cytotoxicity activity of extract and fraction isolated from *Phomopsis* sp.

Sample	Mortality (%) 10 µg/mL	100 µg/mL	1000 µg/mL	LC_{50} (µg/mL)
E	36.67±20.82	100.00±0.00	100±0	6.88
F1	76.67±11.54	96.67±5.77	100±0	2.33
F2	16.67±5.77	30.00±26.46	100±0	48.28
F3	13.33±5.77	30.00±17.32	100±0	50.56
F4	10±0.00	26.67±15.28	100±0	55.78
F5	6.67±5.77	30.00±10.00	100±0	80.84
F6	23.33±5.77	33.33±5.77	100±0	40.10
F7	6.67±11.54	46.67±15.27	100±0	95.05
F8	0.00±0.00	13.33±5.77	37±6	843.50
F9	6.67±5.77	10.00±0.00	70±20	482.79
F10	3.33±5.77	10.00±10.00	40±10	1644.31

E= ethyl acetate extract; Fn=fraction n, for example F1 = fraction I

F1 anticancer activity in MCF-7 cells

Trypan blue was used as the exclusion dye in the anti-proliferation cell assay. This method is based on the principle that live cells possess intact cell membranes capable of excluding certain dyes, such as trypan blue. A viable cell will have a clear cytoplasm, while non-viable cells tend to have a blue cytoplasm.[39] Data from Table 2 were constructed using the regression line equation model y = ax + b. Figure 1 shows the relationship between concentration and % inhibition for MCF-7 cells, and Figure 2 presents the same for Vero cells. The equation model for MCF-7 was y = −13.811x + 128.05, and that for Vero was y = −10.961x + 107.1. These equations were then used to determine the IC_{50} values.

Aside from the LC_{50}, another cytotoxicity measure is the IC_{50}. The NCI states that an IC_{50} < 20 µg/mL shows a very high potential as an anticancer drug [40]. F1 had an IC_{50} of 5.65 µg/mL, suggesting high cytotoxicity. Compared to TAM at the same concentration (4 µg/mL), F1 showed greater inhibition (92.97 %) than TAM (77.64 %). The concentration of F1 also showed more antiproliferation activity in MCF-7 than *Phomopsis* sp. extract in the previous study at 19.20 µg/mL.[10] In comparison, Santos *et al.* [41] found that *Phomopsis* sp. from *Casearia arborea* Rich leaves had IC_{50} of 49.2 µg/mL in MCF-7. The results showed the potent cytotoxic effects of *Phomopsis* sp. extract on MCF-7 cells. Fractionation improves the purity of a compound, which can in turn increase the activity of a sample.[41]

ISSN 2616-0684 (Print)
ISSN 2616-0692 (Electronic)

Table 2: Inhibition activity of F1 purified from *Phomopsis* sp. extract against human breast cancer (MCF-7) and normal Vero cell lines

Sample	Concentration (µg/mL)	Inhibition activity (%)		IC_{50} (µg/mL)	
		MCF-7	Vero	MCF-7	Vero
F1	32	99.36±0.55	91.41±1.25	5.65	5.21
	16	98.40±0.55	87.44±1.51		
	8	96.49±0.55	81.82±2.06		
	4	92.97±3.99	61.32±15.96		
	2	71.57±20.34	47.93±3.93		
	1	19.49±10.14	42.48±7.79		
Tamoxifen	4	77.64±7.26	63.14±10.59		

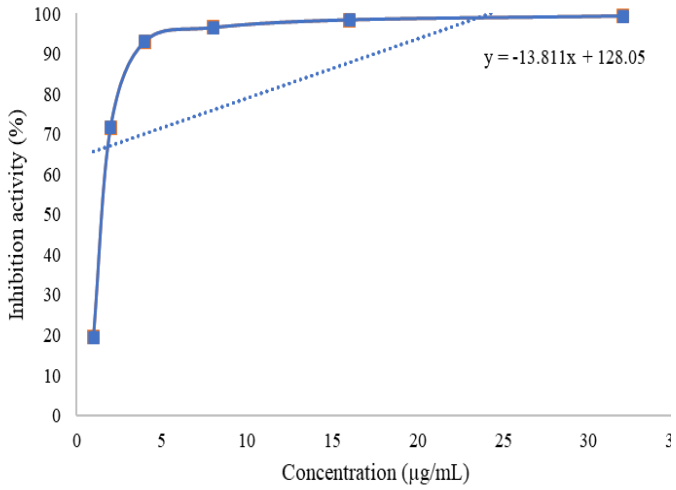

Figure 1: The curve correlations between sample concentration and MCF-7 cell inhibition

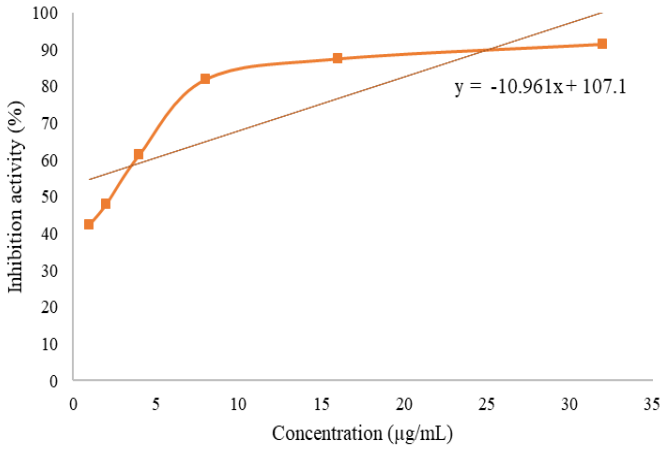

Figure 2: The curve correlations between sample concentration and Vero cell inhibition

This study evaluated the antiproliferative activity of F1 in normal Vero cells. At the same concentration (4 µg/mL), F1 showed slightly lower inhibition (61.32%) than TAM (63.14%), indicating reduced cytotoxicity toward normal cells. Although F1 showed significant activity against Vero cells (IC_{50} = 5.21 µg/mL), which is markedly lower than the value reported by Ahamed and Murugan for a related fraction (66 µg/mL),[42] the inhibitory effect remained lower than TAM under the same conditions. The difference in cytotoxic values may be influenced by the distinct sources of the endophytic fungi, as the *Phomopsis* sp. examined by Ahamed and Murugan [42] was isolated from marine algae. According to Alam et al., [43], endophytic fungi are capable of producing different secondary metabolites depending on the host organism. Chemical variations in the host, particularly those induced by environmental stress, can further modulate secondary metabolite biosynthesis in the associated endophytes.

TAM also inhibits cell-cycle progression by modulating key regulatory proteins, including cyclins, thereby preventing the transition from the G1 to the S phase [44]. However, a major limitation of this drug is the development of resistance, which is partly driven by estrogen-mediated increases in the Bcl-2:Bax ratio, known to promote cell survival. HER-2 overexpression also enhances the levels of anti-apoptotic proteins Bcl-2 and Bcl-xL, resulting in reduced tamoxifen-induced apoptosis and further contributing to tamoxifen resistance[45]. These results suggest that F1 is still comparatively safer for normal cells than the commercial drug TAM.

Inducing apoptosis

The morphology of MCF-7 cells was examined using a fluorescence microscope following acridine orange–ethidium bromide (AO/EB) staining to assess the apoptotic activity induced by *Phomopsis* sp. F1 fraction. AO permeates intact cell membranes and intercalates with nuclear DNA, producing green fluorescence in viable cells. In contrast, EB enters cells only after the loss of cytoplasmic membrane integrity and stains the nucleus red, serving as an indicator of apoptotic or necrotic processes. Based on these fluorescence characteristics, normal viable cells show uniformly green nuclei, early apoptotic cells are characterized by green nuclei with condensed or fragmented chromatin, late apoptotic cells present orange nuclei with highly condensed and fragmented chromatin, and necrotic cells have orange-red nuclei with morphologically normal chromatin [46].

The negative control with untreated MCF-7 cells showed normal cell morphology with a bright green fluorescent color (Figure 3A). TAM, as a positive control, produced necrotic cells with normally shaped, orange-red, and unfragmented nuclei (Figure 3B). Treatment with F1 changed the morphology of MCF-7 cells, inducing apoptosis, as shown by the rupture and disintegration of the nucleus and shrinking of the cytoplasm (Figure 3C).

TAM (positive control) is a cancer drug that acts as a selective estrogen receptor modulator (SERM).[47] It competitively binds to 17β-estradiol (E2) at the estrogen receptor site in tumors and other target tissues to produce a nuclear complex that reduces DNA synthesis, inhibiting the development of breast cancer.[48] Long-term TAM use can lead to resistance caused by estrogen, thereby increasing the Bcl-2:Bax ratio. Additionally, HER-2 overexpression increases the expression of the anti-apoptotic proteins Bcl-2 and BclxL, which decreases TAM-triggered apoptosis and increases TAM resistance.[49]

To assess the impact of F1 on apoptosis in MCF-7 cells, their morphology was examined using AO–EB staining under a microscope. The findings indicated that F1 induced cell death in MCF-7 cells at a concentration of 5 µg/mL. This is consistent with Hadisaputri *et al.*[50], who found that nuclear fragmentation, disruption of the cytoplasm, and formation of apoptotic bodies are hallmarks of apoptotic cells. According to Wang et al.,[51], compounds in the extract of

ISSN 2616-0684 (Print)
ISSN 2616-0692 (Electronic)

Phomopsis sp. can induce apoptosis by repairing mitochondrial function and inducing both ER stress and the mitochondrial apoptotic pathway.

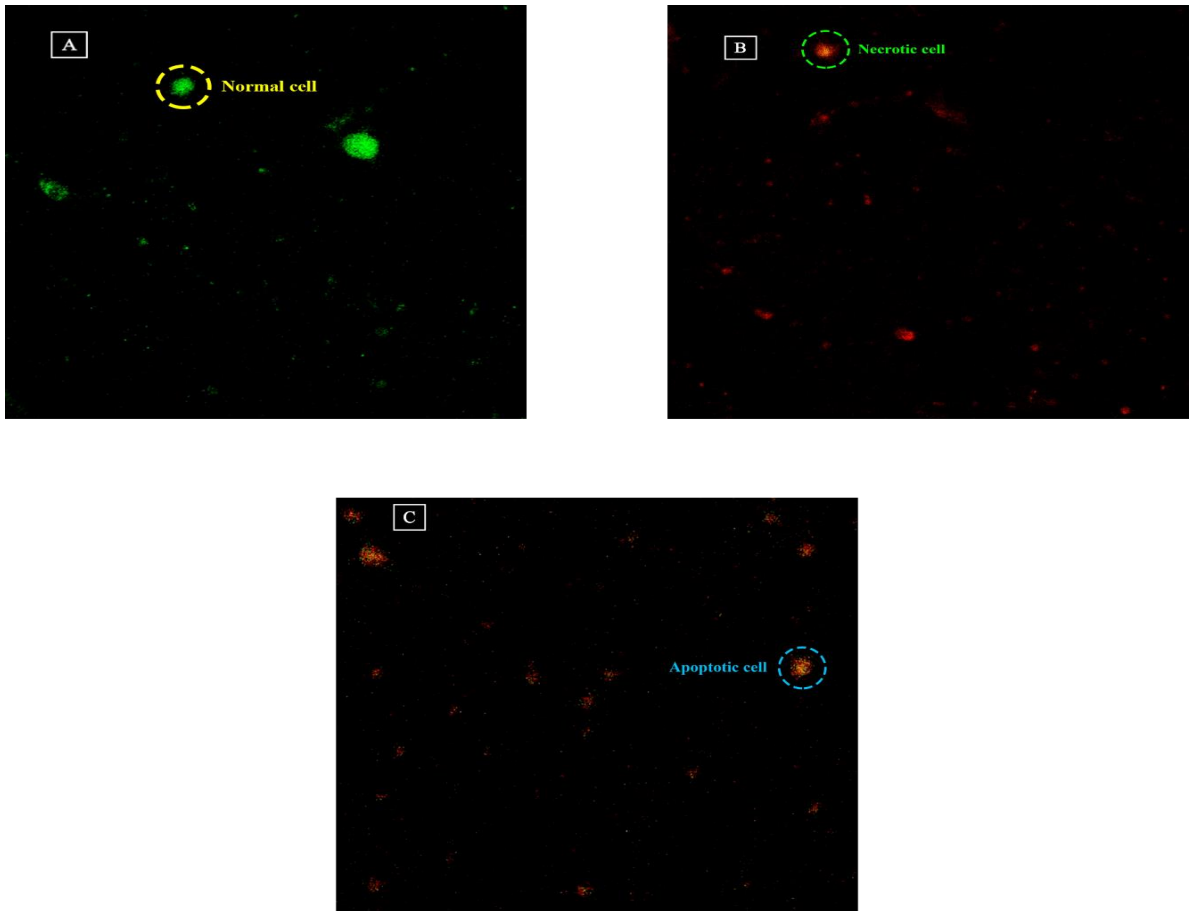

Figure 3: Fluorescence microscopy analysis of cell death profiles following treatment. (A) Negative control showing predominantly viable (normal) cells with green fluorescence. (B) Tamoxifen-treated cells exhibiting necrotic characteristics, indicated by red fluorescence. (C) Cells treated with F1 fraction of *Phomopsis* sp., showing apoptotic features characterized by condensed and fragmented fluorescence signals. Representative normal, necrotic, and apoptotic cells are indicated by dashed circles

Compound identification with LC−MS/MS

This study identified both known and unknown compounds (not listed in the database used) in the F1 soursop leaf endophytic fungus sample, with more unknown than known compounds. Among the 38 total compounds, there were only 9 known, as shown in Table 3 and Figure 4. Two novel compounds discovered in *Phomopsis* sp., cytosporone C and phomochromone B, have been previously discovered by other studies and share similarities with known compounds.[52,53] The identified compounds considered to have potential anticancer activity include kynurenic acid [54], maraniol [55], (-)-caryophyllene oxide [56], and chalcone.[57,58] However, it is possible that unknown compounds may also have anticancer activity.

Table 3: Identified compounds of F1 with Liquid Chromatography-tandem with Mass Spectrometry (LC-MS/MS)

No	Retention time	Molecular weight (m/z)	Estimation compound (internal database)	Molecular formula	Percent composition (%)	Estimated compound (references)
1	21.54	278.1518	Diisobutylphthalate	$C_{16}H_{22}O_4$	21.35	Cytosporone C [53]
2	29.47	390.2770	Bis(2-ethylhexyl) phthalate	$C_{24}H_{38}O_4$	17.66	
4	21.54	189.0426	Kynurenic acid	$C_{10}H_7NO_3$	1.65	
5	21.59	204.0786	Maraniol	$C_{12}H_{12}O_3$	1.39	
6	22.22	220.1827	(-)-Caryophyllene oxide	$C_{15}H_{24}O$	0.30	
7	21.53	222.0889	Monobutyl phthalate	$C_{12}H_{14}O_4$	0.22	Phomochromone B [52]
8	28.59	376.2614	3beta,17beta-Diacetoxy-5alpha-androstane	$C_{23}H_{36}O_4$	0.21	
9	18.22	208.0888	Chalcone	$C_{15}H_{12}O$	0.18	

ISSN 2616-0684 (Print)
ISSN 2616-0692 (Electronic)

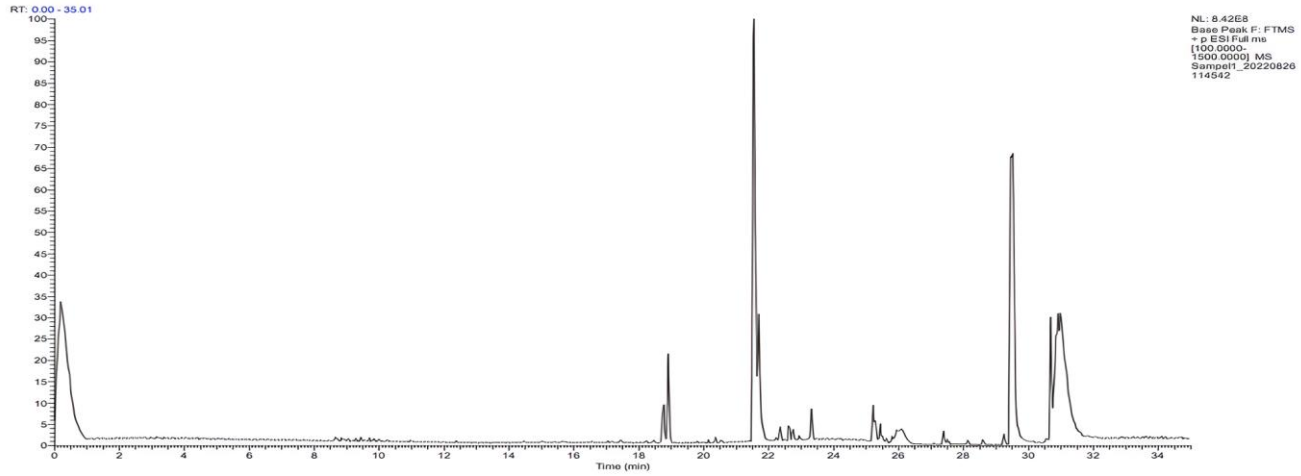

Figure 4: Chromatogram of the F1 soursop leaf *Phomopsis* sp. fractions

The analysis of F1 showed the presence of both known and unknown compounds. Cytosporone C, a previously identified *Phomopsis* sp. compound, shares similarities with diisobutylphthalate (m/z = 278.1518). Monobutyl phthalate (m/z = 222.0892) and phomochromone B (m/z = 222.0892) were discovered by Ahmed *et al.*[52]. Cytosporone C, kynurenic acid, maraniol, (-)-caryophyllene oxide, and chalcone have shown potential as anticancer drugs through apoptotic cell-killing mechanism.[17,54–56,58–61]

Cytosporone C is a relatively novel compound in *Phomopsis* sp., but the mechanism of cytotoxicity has not been identified. In the study by Kongprapan et al.,[61], the compound showed good cytotoxicity against MCF-7 and KB cells (IC_{50} = 19.11 and 12.68 µg/mL, respectively). Additionally, it showed antibacterial activity against two fungi, *Fusarium oxysporum* and *Candida albicans* (MIC = 115.1–198.8 µM).[59]

Kynurenic acid, a key metabolite derived from tryptophan, is synthesized via the kynurenine pathway, influencing the immune system, inflammation, and cancer.[62] While the comprehensive mechanism remains unclear, earlier research has suggested its potential role as an endogenous agonist of AhR, which is involved in various processes such as cell proliferation, apoptosis, adipose differentiation, tumor suppression, and immune cell differentiation.[63] The heightened production of apoptotic markers like FasL, Fas, caspase-3, and 8 also indicates apoptosis. Furthermore, anti-apoptotic factors such as PI3K, AKT, and Bcl-xL modulate apoptosis-inducing elements like BAD, Bak, Bax, cytochrome C, and caspase 9.[54]

Maraniol (7-Ethoxy-4-methylcoumarin) is a coumarin derivative that shows anticancer activity in molecular docking experiments.[55] Coumarin has several mechanisms, including the reduction of carbon anhydrate, inhibition of tumor angiogenesis, activation of the PI3K/Akt/mTOR pathway, and apoptotic proteins.[64]

One sesquiterpenoid oxide, (-)-caryophyllene oxide, is often known as beta-caryophyllene oxide (BCPO). Lei et al., [56] reported the ability to reduce oxidative stress while increasing apoptosis and antioxidant activity. BCPO also induces the PI3K/AKT/mTOR/S6K1 signaling pathway, which is important in cell survival, proliferation, and tumor angiogenesis.[56,60]

Chalcone, as secondary metabolites within the flavonoid family (C6-C3-C6 system), are widely found in both edible and medicinal plants, serving as key precursors for the biosynthesis of plant flavonoids. The unique and simple chemical structure enables it to replace abundant hydrogen atoms, resulting in high biological activity.[65] The flexible structure of chalcone also contributes to the ability to bind many enzymes and receptors. For instance, 1,2,4-triazole chalcone has been reported to induce apoptosis by increasing Bax and activating caspases 3, 8, and 9.[58]

After successfully conducting *in vitro* tests to show the anti-breast cancer potential of soursop leaf extract infected with endophytic fungus F1, computational *in silico* studies were conducted to explore and understand the mechanisms of action for bioactive compounds within the extract. This method provides a solid scientific foundation for laboratory results.

Computational in silico analysis

PASS analysis

During the initial stage of the *in silico* study, researchers examined the biological activity of these compounds by analyzing their structural formulas. The primary focus was on their potential to combat breast cancer, determined by a Probability to be Active (Pa) value that needed to surpass the Probability to be Inactive (Pi) value. As indicated in Table 4, TAM, a widely recognized treatment for breast cancer, exhibited a Pa value of 0.817 and a Pi value of 0.004. Therefore, compounds with Pa values approaching those of TAM were predicted to show similar anti-breast cancer properties. Several drug candidates, including chalcone, benzophenone A, and 3beta,17beta-Diacetoxy-5alpha-androstane, showed Pa values close to that of TAM.

Table 4: Predicted biological activity data from PASS regarding its anti-breast cancer activity

Compounds	Pa value	Pi value
Chalcone	0.544	0.015
(-)-Caryophyllene oxide	0.494	0.019
Benzophomopsin A	0.641	0.008
Diisobutylphthalate	0.273	0.063
Phomochromone B	0.226	0.082
3beta,17beta-Diacetoxy-5alpha-androstane	0.551	0.014
Bis(2-ethylhexyl) phthalate	None	None
Kynurenic acid	0.171	0.115
Tamoxifen (Positive Control)	0.817	0.004

Initially, this study validated the biological activity of compounds identified by LC-MS/MS as anti-breast cancer agents based on laboratory tests using the PASS online tool. This open-access server has been widely used to analyze the chemical structures of compounds intended as drug candidates and predict the potential biological activity. PASS prediction tools were developed using 20.000 PCs and approximately 4.000 types of biological activity, relying on structural formulas and achieving an average accuracy of approximately 90% [66,67]. The results showed that the compounds derived from the soursop leaf extract infected with endophytic fungus F1 had pharmacological potential against breast cancer, as indicated by a Pa value greater than Pi. A previous study using the PASS online approach for anti-breast cancer screening was conducted by Sehrawat et al., [68], who successfully formulated potent inhibitors for breast cancer treatment using a range of methodologies, including PASS online.

Molecular docking

To analyze the interactions between proteins and ligands and evaluate the binding energies of drug candidates to the Erα protein, *in silico* molecular docking methods were used. As presented in Table 5, the results showed that the drug candidates possessed binding energies ranging from 6.958 to 8.392 kcal/mol. TAM, a standard treatment for breast cancer, had a binding energy of 6.794 kcal/mol. The binding energy values of the drug candidates were found to be superior to those of TAM, according to predictions made using *in silico* molecular docking methods. This result provides compelling evidence that drug candidates derived from F1 soursop leaf endophytic fungal samples possess significant potential as anti-breast cancer agents.

Table 5: Molecular docking data of compounds from the F1 soursop leaf endophytic fungus as inhibitors of the Erα protein

Rank	CID	Compounds	Binding energy (kcal/mol)
1	637760	Chalcone	8.392
2	1742210	(-)-Caryophyllene oxide	8.252
3	44513691	Maraniol	7.756
4	10778975	Diisobutylphthalate	7.697
5	52953426	Phomochromone B	7.244
6	224008	3beta,17beta-Diacetoxy-5alpha-androstane	7.212
7	6441416	Ergosta-4,6,8(14),22-tetraen-3-one	7.075
8	8343	Bis(2-ethylhexyl) phthalate	7.047
9	3845	Kynurenic acid	6.958
10	2733526	Tamoxifen (positive control)	6.794

ADMET/Pharmacokinetics Studies

The properties and profiles of absorption, distribution, metabolism, elimination, and toxicity (ADMET/pharmacokinetics) of each compound derived from the F1 soursop leaf endophytic fungus sample were predicted using the SwissADME server. The extracted data from this server, presented in Table 6, show that the molecular weights of the compounds were relatively low, ranging from 120 to 392.62 g/mol. Compounds with lower molecular weights were predicted to have favorable absorption and distribution properties. This correlates with the gastrointestinal absorption of the drug candidates, suggesting that all molecules may be easily absorbed through the digestive tract. Furthermore, all drug candidates showed good oral bioavailability according to Lipinski's rule of five. SwissADME predictions also showed that none of the compounds were probable to cause liver injury.

In terms of pharmacokinetics, the number of hydrogen bond acceptors and donors provides insights into the potential interactions of a compound within biological systems. Based on the results, all compounds possessed at least one hydrogen bond acceptor, although some compounds, including chalcone, (-)-caryophyllene oxide, 3beta,17beta-diacetoxy-5alpha-androstane, and bis(2-ethylhexyl) phthalate, did not contain any hydrogen bond donors. Finally, the quantitative predictive data showed that only a few compounds showed ease of synthesis, with a lower numerical value showing greater synthetic feasibility. Overall, the predictions suggest that all drug candidates are relatively safe and viable as potential therapeutic agents based on the analyses conducted by SwissADME.

Following the ADMET/pharmacokinetic predictions, the chalcone candidate was further investigated due to the favorable synthetic accessibility. The protein-chalcone complex was examined using the protein-tamoxifen complex as a comparative reference for analyzing the output data.

Table 6: Predicted ADMET/pharmacokinetics data generated by SwissADME for the F1 soursop leaf endophytic fungus

Compounds	Molecular Weight (g/mol)	Num. H-bond acceptors	Num. H-bond donors	TPSA (Å²)	GI Absorption	Bioavailability Score	Lipinski	Liver Injury I	Synthetic accessibility
Chalcone	208.26	1	0	17.07	High	0.55	Yes	Safe	2.41
(-)-Caryophyllene oxide	220.35	1	0	12.53	High	0.55	Yes	Safe	4.35
Benzophomopsin A	204.22	3	1	41.99	High	0.55	Yes	Safe	4.37
Diisobutylpht	278.34	4	2	66.76	High	0.55	Yes	Safe	3.47

ISSN 2616-0684 (Print)
ISSN 2616-0692 (Electronic)

halate									
Phomochromone B	222.24	4	2	66.76	High	0.55	Yes	Safe	3.55
3beta,17beta-Diacetoxy-5alpha-androstane	376.53	4	0	52.60	High	0.55	Yes; 1 violation: MLOGP >4.15	Safe	4.52
Bis(2-ethylhexyl) phthalate	390.56	4	0	52.60	High	0.55	Yes; 1 violation: MLOGP >4.15	Safe	4.12
Kynurenic acid	189.17	3	2	70.16	High	0.85	Yes	Toxic	1.59

Post-docking analysis

The interactions within the selected protein-ligand complexes were analyzed by visualizing the complexes, as shown in Figure 5. The Erα protein possesses an active pocket composed of the amino acid residues Trp383, Ala350, Asp351, Phe404, and Leu387. TAM interacts with the Erα protein through several hydrogen and hydrophobic bonds. Hydrogen bonds are formed between TAM and the amino acid residues Ile326, Gly390, and Ile386 in Erα. These hydrogen bonds arise from the hydroxyl (–OH) groups on the TAM molecule interacting with the corresponding atoms in the Erα protein, with bond distances ranging from 2.04 to 3.05 Å. Additionally, attractive charge interactions with Glu353 were observed, and hydrophobic interactions occurred between TAM and the amino acid residues Trp393 and Pro324.

The Erα-chalcone complex is particularly significant, as the visualization shows hydrophobic interactions between chalcone and two amino acid residues within the active pocket, specifically Ala350 and Leu387, with bond distances of 4.65 Å and 4.63 Å, respectively. This complex showed the highest binding energy compared to the control drug, TAM, and other drug candidates, which was attributed to hydrophobic interactions. However, hydrogen bonds were absent in this complex. Despite the lack of hydrogen bonds in the Erα-chalcone complex compared to the Erα-tamoxifen complex, chalcone can still interact with the Erα protein stably and strongly, resulting in effective inhibition. The analysis data for both protein-ligand complexes are presented in Table 7.

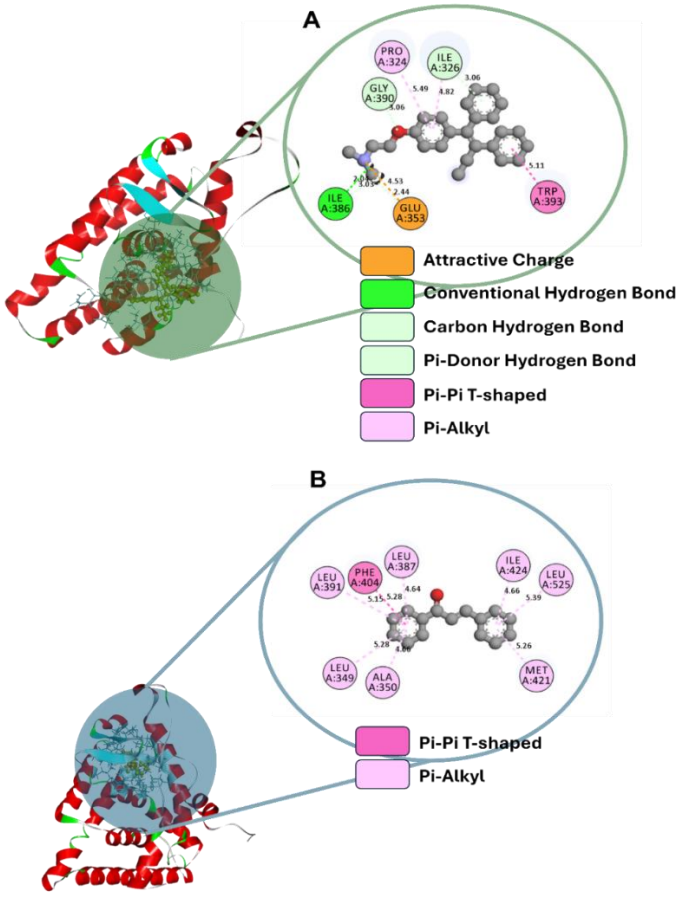

Figure 5: 2D and 3D visualizations of compound interactions with Erα, showing various types of bonds formed with the amino acid residues of the Erα protein. A) Erα-tamoxifen complex. B) Erα-chalcone complex

ISSN 2616-0684 (Print)
ISSN 2616-0692 (Electronic)

Table 7: Interactions of Erα-tamoxifen and Erα-chalcone complexes

Complex Enzyme-Ligand	Name	Distance (Å)	Category	Types	From	From chemistry	To	To Chemistry
Erα - Tamoxifen	A:UNK5:N - A:GLU353:OE1	4.52	Electrostatic	Attractive Charge	A:UNK5:N	Positive	A:GLU353:OE1	Negative
	A:UNK5:H - A:ILE386:O	2.04	Hydrogen Bond	Conventional Hydrogen Bond	A:UNK5:H	H-Donor	A:ILE386:O	H-Acceptor
	A:GLY390:HA1 - A:UNK5:O	3.05	Hydrogen Bond	Carbon Hydrogen Bond	A:GLY390:HA1	H-Donor	A:UNK5:O	H-Acceptor
	A:UNK5:H1 - A:ILE386:O	3.03	Hydrogen Bond	Carbon Hydrogen Bond	A:UNK5:H1	H-Donor	A:ILE386:O	H-Acceptor
	A:UNK5:H2 - A:GLU353:OE1	2.44	Hydrogen Bond	Carbon Hydrogen Bond	A:UNK5:H2	H-Donor	A:GLU353:OE1	H-Acceptor
	A:ILE326:H - A:UNK5	3.05	Hydrogen Bond	Pi-Donor Hydrogen Bond	A:ILE326:H	H-Donor	A:UNK5	Pi-Orbitals
	A:TRP393 - A:UNK5	5.10	Hydrophobic	Pi-Pi T-shaped	A:TRP393	Pi-Orbitals	A:UNK5	Pi-Orbitals
	A:UNK5 - A:PRO324	5.48	Hydrophobic	Pi-Alkyl	A:UNK5	Pi-Orbitals	A:PRO324	Alkyl
	A:UNK5 - A:ILE326	4.81	Hydrophobic	Pi-Alkyl	A:UNK5	Pi-Orbitals	A:ILE326	Alkyl
	A:UNK5 - A:ILE326	5.00	Hydrophobic	Pi-Alkyl	A:UNK5	Pi-Orbitals	A:ILE326	Alkyl
Enzyme-Chalcone	A:PHE404 - A:UNK10	5.27	Hydrophobic	Pi-Pi T-shaped	A:PHE404	Pi-Orbitals	A:UNK10	Pi-Orbitals
	A:UNK10 - A:LEU349	5.27	Hydrophobic	Pi-Alkyl	A:UNK10	Pi-Orbitals	A:LEU349	Alkyl
	A:UNK10 - A:ALA350	4.65	Hydrophobic	Pi-Alkyl	A:UNK10	Pi-Orbitals	A:ALA350	Alkyl
	A:UNK10 - A:LEU387	4.63	Hydrophobic	Pi-Alkyl	A:UNK10	Pi-Orbitals	A:LEU387	Alkyl
	A:UNK10 - A:LEU391	5.14	Hydrophobic	Pi-Alkyl	A:UNK10	Pi-Orbitals	A:LEU391	Alkyl
	A:UNK10 - A:MET421	5.25	Hydrophobic	Pi-Alkyl	A:UNK10	Pi-Orbitals	A:MET421	Alkyl
	A:UNK10 - A:ILE424	4,65801	Hydrophobic	Pi-Alkyl	A:UNK10	Pi-Orbitals	A:ILE424	Alkyl
	A:UNK10 - A:LEU525	5,38651	Hydrophobic	Pi-Alkyl	A:UNK10	Pi-Orbitals	A:LEU525	Alkyl

ISSN 2616-0684 (Print)
ISSN 2616-0692 (Electronic)

Following the identification of the anti-breast cancer pharmacological effects through PASS online, the results were validated using *in silico* docking studies. Previous studies have shown that docking is effective in the early stages of drug discovery. *In silico* docking serves as a crucial method in drug design to predict how a ligand (a potential drug) interacts with its target protein receptor.[69] This study provides evidence that all ligands show potential as candidate inhibitors, as indicated by the more positive binding energy values compared to TAM, which is the reference for binding energy and other characteristics. Post-docking analysis showed that hydrogen bonds were absent in the Erα-chalcone complex, while hydrogen bonds were present in the Erα-tamoxifen complex. Through docking studies, Hussein et al.,[70], showed that hydrogen bonding and hydrophobic interactions contribute to the stability of the protein-ligand complex. In addition, indications of improved binding energies were observed.

DFT analysis

The HOMO and LUMO energies can be used to obtain data on the ability of the molecules to donate or accept electrons. Figure 6 shows the HOMO, LUMO, and energy gap values. Based on these calculations, TAM showed a LUMO energy of -0.02689 eV, HOMO energy of -0.19207 eV, and energy gap of -0.16518 eV, while chalcone had values of -0.07774 eV, -0.23272 eV, and -0.15498 eV, respectively. The difference between these two energies, or the energy gap, shows the stability and reactivity of a molecule. Despite the slightly higher energy gap than TAM (positive control), chalcone is considered a promising candidate due to the energy gap difference of 0.0102 eV.

The ionization potential (I), electron affinity (A), chemical potential (μ), electronegativity (χ), hardness (η), softness (S), and electrophilicity index (ω) were calculated based on the LUMO and HOMO orbital energies, as presented in Table 8. The results showed that chalcone showed favorable reactivity similar to the control drug TAM.

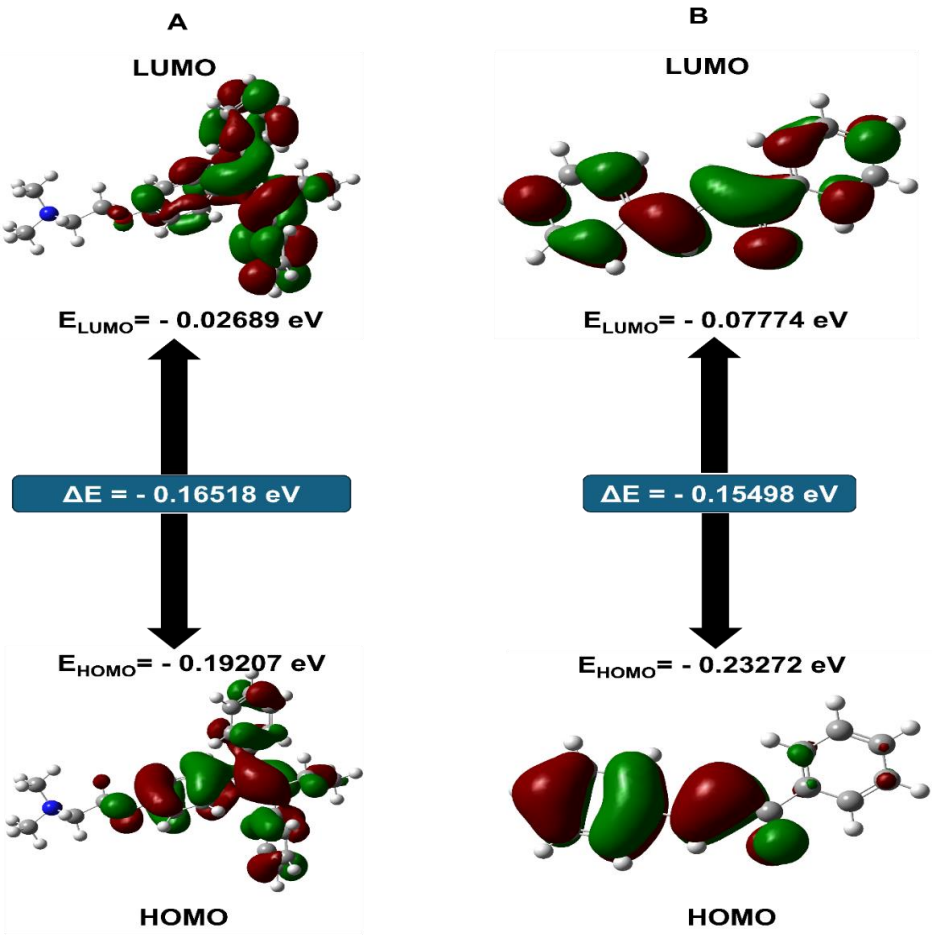

Figure 6: Visualization and predicted data of HOMO energy, LUMO energy, and energy gap for the control drug and selected candidate drugs (A) Tamoxifen (B) Chalcone

Table 8: DFT-calculated HOMO–LUMO energies, energy gap, and molecular properties

Compounds	Homo (eV)	Lumo (eV)	Energy gap (eV)	Ionization potential (I) (eV)	Electron affinity (A) (eV)	Chemical potentials (μ) (eV)	Electronegativity (χ) (eV)	Hardness (η) (eV)	Softness (S) (eV)	Electrophilicity index (ω) (eV)
Tamoxifen	- 0.19207	- 0.02689	- 0.16518	0.19207	0.02689	-0.10948	0.10948	0.08259	6.05400	0.07256
Chalcone	- 0.23272	- 0.07774	- 0.15498	0.23272	0.07774	-0.15523	0.15523	0.07749	6.45245	0.15548

ISSN 2616-0684 (Print)
ISSN 2616-0692 (Electronic)

This study also incorporated DFT analysis, a computational method used to understand the molecular structures by examining the energies of the orbitals. DFT quantitatively explains how structural changes in molecules influence biological activity and aids in analyzing compounds predicted to have specific effects in biological systems. This method is grounded in the Hohenberg-Kohn theorem, broadly stating that electron density can determine the properties of a molecule.[71]

Post-MD analysis

After conducting several analyses based on previous methods, *in silico* docking tests were performed on the selected complexes, Erα-chalcone and the control Erα-tamoxifen. MD simulations were then executed over a trajectory of 300 ns to examine the conformational stability and analyze the dynamic properties of the protein-ligand complexes. Various calculations were used to analyze the post-MD data, including the RMSD of C-alpha, radius of gyration (Rg), hydrogen bonds, SASA, RSMF, and binding energy.

The stability of both protein-ligand complexes was evaluated using the RMSD of C-alpha (Figure 7A). The results showed that the Erα-chalcone complex had a lower average RMSD C-alpha value (3.121 Å) than the Erα-tamoxifen complex (3.175 Å), suggesting reduced structural fluctuations in the Erα-chalcone complex. The 300 ns MD simulation trajectory was divided into three segments, namely 0-100 ns, 100.25-200 ns, and 200.25-300 ns. The average RMSD C-alpha values were calculated for each segment to assess the equilibrium attainment. A decrease or stability in the average RMSD C-alpha values from one segment to the next showed an improvement in system stability.

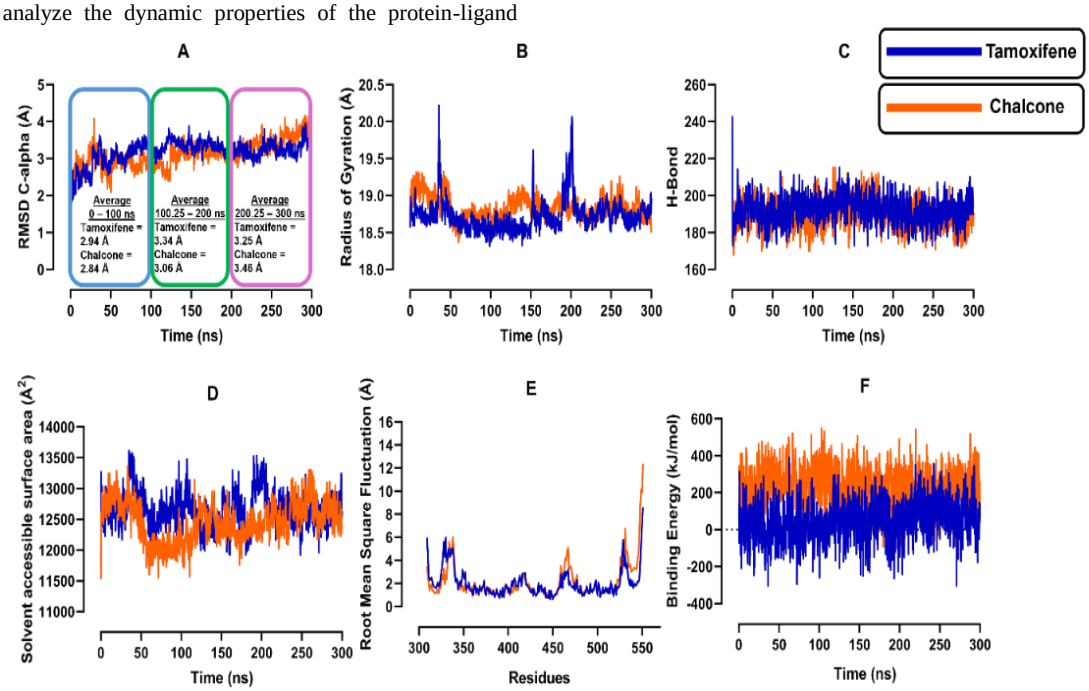

Figure 7: Data from the 300 ns molecular dynamics (MD) simulation presented in graphs showing various analyses throughout the simulation (A) C-alpha RMSD (B) Radius of gyration (C) Hydrogen bonds (D) SASA (E) RMSF (F) Binding energy

In the Erα-tamoxifen complex, an increase in the average RMSD of C-alpha was observed from segment 1 to segment 2, suggesting that the system may not have reached equilibrium in the early stages. However, a decrease in the average RMSD C-alpha from segments 2 to 3 showed that the system might approach equilibrium, although with continuous fluctuations. The Erα-chalcone complex, on the other hand, showed a significant increase in average RMSD across all segments (segment 1:2.84 Å, segment 2:3.06 Å, and segment 3:3.46 Å). This suggests the presence of more significant fluctuations or conformational changes in this complex during the simulation than in Erα-tamoxifen, which may affect stability. Overall, the chalcone complex showed similarities to the commercial ligand tamoxifen. To achieve a more comprehensive analysis of the stability of both complexes, further evaluation using parameters other than RMSD C-alpha is necessary.

Figure 7B shows the Rg plot for both complexes during the 300 ns simulation. The stability of Rg, indicated by minimal fluctuations and low average values, correlates with the stability of the protein throughout the 300 ns simulation. Evaluating Rg enables better understanding and measurement of the compactness of the protein structure during MD simulation. Based on this analysis, the Erα-tamoxifen complex showed slightly better compactness, with an average Rg value of 18.723 Å, compared to Erα-chalcone, with an average Rg of 18.843 Å.

Further analysis of the Rg data showed that the Erα-chalcone complex reached a peak value of 20.216 Å at 35.75 ns, while Erα-tamoxifen recorded an Rg value of 18.988 Å at the same time point. This observation suggests that the interaction of chalcone with Erα may slightly influence the protein-folding mechanism at the onset of the simulation. The Rg plot for the Erα-tamoxifen complex (blue line in Figure 7B) also showed greater fluctuations at several points during MD simulation. In contrast, the Rg plot for the Erα-chalcone complex (orange line in Figure 7B) showed relatively smaller fluctuations than those for the Erα-tamoxifen complex. Based on this Rg plot, the Erα-chalcone complex is less prone to fluctuations than the commercial ligand Erα-tamoxifen. However, TAM tends to have a more stable average Rg throughout the simulation period than chalcone.

The interactions of chalcone and tamoxifen with Erα were further evaluated by calculating the hydrogen bond profile during the 300 ns MD simulation. Figure 7C shows that both chalcone and TAM formed hydrogen bonds with Erα. The average number of hydrogen bonds formed was 192.57 for TAM and 190.25 for chalcone. These results are consistent with previous *in silico* molecular docking results, showing that the Erα-tamoxifen complex had more hydrogen bonds than Erα-chalcone. The increased internal hydrogen bonding within the complexes suggests enhanced structural stability, which implies a reduction in solute-solvent hydrogen interactions.

To further explore the interactions between the complexes and solvent during the 300 ns MD simulation, SASA analysis was conducted. A plot of the SASA production data is presented in Figure 7D. The Erα-tamoxifen complex produced SASA data with an average of 12.649.6 Å², while Erα-chalcone had an average of 12.458.6 Å². Although chalcone showed a slightly higher SASA, neither compound demonstrated statistically significant differences in SASA values.

ISSN 2616-0684 (Print)
ISSN 2616-0692 (Electronic)

SASA is a parameter used to predict protein folding because it reflects the potential exposure of the protein surface to the surrounding solvent. A greater surface area exposed to the solvent shows a reduced folding capacity of the protein, which may lead to destabilization of the hydrophobic regions.

To assess the flexibility of the amino acid residues within the protein-ligand complexes, particularly in the active pocket of protein Erα (Trp383, Ala350, Asp351, Phe404, and Leu387), RMSF analysis was used. The RMSF analysis results (Figure 7E) showed that TAM induced greater flexibility in most active pocket residues, with RMSF values of 2.713 Å for Ala350 and 2.417 Å for Asp351, compared to chalcone, which had RMSF values of 1.328 Å and 1.662 Å, respectively. However, chalcone induced slightly higher flexibility in Leu387, with an RMSF value of 1.534 Å, compared to TAM RMSF of 1.469 Å. The results showed that although chalcone induced lower flexibility in the active pocket residues than tamoxifen, it specifically enhanced the flexibility at Leu387.

In the post-MD analysis, the binding energy was calculated using the MM-PBSA method to evaluate the interaction strength between each ligand (tamoxifen and chalcone) and the target protein Erα, throughout the 300 ns MD simulation. In the binding energy calculations conducted using the YASARA software, a more positive binding energy value shows a stronger binding affinity. Calculations showed that the Erα-tamoxifen complex had an average binding energy of 45.598 kJ/mol, while Erα-chalcone had an average binding energy of 227.069 kJ/mol (Figure 7F). Consequently, chalcone with more positive binding energies showed stronger binding affinities for Erα protein. The positive binding energy resulting from the long-term MD simulation (300 ns) suggests favorable stability of the Erα-chalcone complex, showing a greater potential for inhibition.

Post-MD analysis showed that chalcone had significant inhibitory effects on Erα protein during the 300 ns MD simulation. This is further supported by the analyzed parameters, particularly higher binding energy values. MD simulations provide comprehensive insights by exploring various changes and behaviors of protein-ligand complexes, while docking studies typically focus on binding interactions and conformational variations. The combination of docking and MD simulations is an effective strategy for identifying drug candidates with potential pharmacological effects.[72]

PCA and DCCM

The PCA analysis results for the Erα-tamoxifen and Erα-chalcone complexes, conducted over a 300 ns MD simulation, showed that the values for PC1 and PC2 of the Erα-tamoxifen complex were 23.88% and 12.43%, respectively, while PC2 and PC3 were 12.43% and 10.94%, respectively. The values for PC1 and PC3 were 23.88% and 10.94%, respectively. Based on the results, the values of PC1, PC2, and PC3 for the Erα-tamoxifen complex were lower than those for Erα-chalcone, as shown in Figure 8. The low cumulative values of the PCs show stability with minimal variability in the simulation complexes. Therefore, the distribution of the Erα-tamoxifen complex was superior to that of Erα-chalcone.

The DCCM analysis results in Figure 9 showed that the Erα-chalcone complex had a more pronounced red coloration than Erα-tamoxifen. This intense red hue served as a visual representation of the data obtained for each complex. Deeper red shading shows greater conformational stability, reflecting minimal perturbations in structural integrity. More importantly, this intense red coloration was observed for residues 50-150.

PCA was used to analyze the movement direction of the Erα protein structure within the system through the Cα fluctuation levels of the complex. Additionally, DCCM analysis was used to determine the correlation of the Cα atom positions with the presence of other atoms in the Erα structure and to assess potential Cα atom dislocations.[73,74] The results present chalcone as a potential anti-breast cancer drug candidate for further testing.

In line with previous studies, chalcone, an important subclass of flavonoids, has been increasingly recognized for the wide-ranging pharmacological activity, particularly the anticancer potential. Although chalcone occur naturally, the limited abundance and inherent structural variability necessitate synthetic modification to achieve reliable and reproducible bioactivity. A previous study by Xu et al., [75] showed that strategic monosubstitution on ring A substantially enhanced cytotoxicity, particularly against K562 cells, underscoring the critical role of structural optimization in improving anticancer efficacy. Accordingly, this study identified two chalcone derivatives that showed statistically significant, concentration-dependent cytotoxic effects, in line with earlier in vitro reports. Complementary computational analyses further strengthened these results. Molecular docking and dynamics simulations showed strong and stable interactions with CDK2 and VEGFR2, consistent with previous evidence that thiophene substitution improves ligand–target binding. Collectively, the convergence of statistical cytotoxicity data and in silico binding profiles reinforces the therapeutic potential of thiophene-based chalcone and underscores the prospect for further optimization and development [76,77].

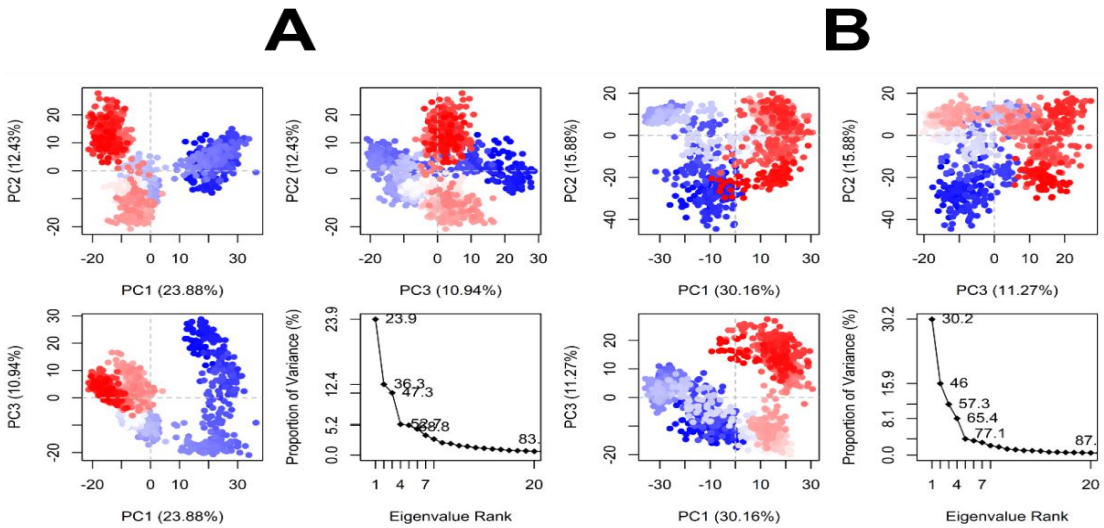

Figure 8: Principal component analysis (PCA) of conformational dynamics of the ERα–ligand complexes: (A) ERα–tamoxifen and (B) ERα–chalcone

ISSN 2616-0684 (Print)
ISSN 2616-0692 (Electronic)

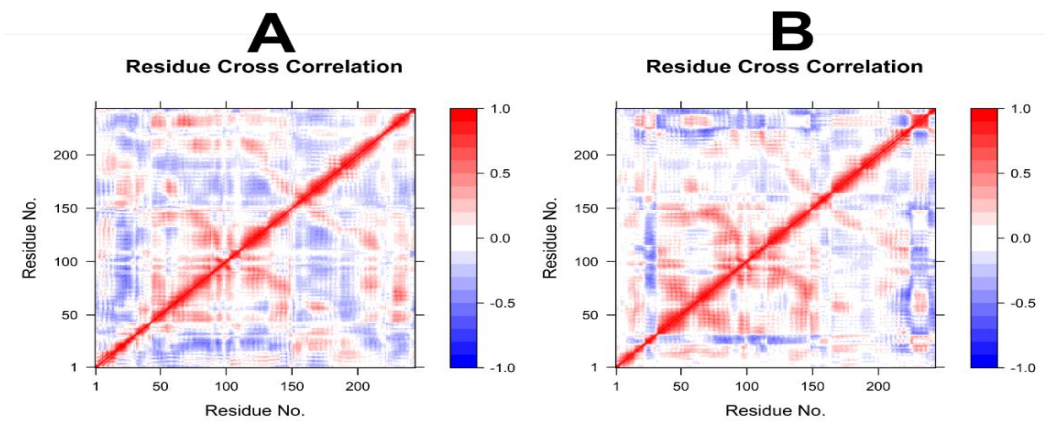

Figure 9: DCCM analysis of conformational changes. A) Erα-tamoxifen complex. B) Erα-chalcone complex

Conclusions

In conclusion, the F1 fraction of *Phomopsis* sp. showed a significant antiproliferative effect on MCF-7 breast cancer cells, with an IC_{50} value of 5.65 µg/mL, indicating the potential as an effective anti-breast cancer agent through the apoptotic pathway. Additionally, the F1 fraction showed significant inhibitory activity in Vero cells, as evidenced by an IC_{50} of 5.21 µg/mL. The identified anticancer compounds, including cytosporone C, kynurenic acid, maraniol, (−)-caryophyllene oxide, and chalcone, were further validated by computational *in silico* studies, suggesting the viability as candidates for breast cancer therapy. However, ADME/pharmacokinetic analyses showed that only a few of these candidates had favorable profiles, with chalcone indicating promising synthetic accessibility. DFT studies and MD simulations further confirmed that chalcone possesses superior properties compared to TAM, enhancing the potential as a therapeutic agent against breast cancer. The results underscore the significance of the soursop leaf endophytic fungi fraction (F1) and the constituents as potential candidates for further exploration in the advancement of effective therapies for breast cancer. This study provides a comprehensive evaluation integrating both in vitro laboratory assays and in silico computational analyses. The results are expected to contribute significantly to the discovery and development of potential breast cancer therapeutic agents while opening avenues for subsequent investigations. Future investigation prospects include optimizing efficacy and safety profiles, exploring oral bioavailability and toxicity parameters, and advancing the work toward in vivo studies using appropriate animal models.

Conflict of Interest

The authors declare no conflict of interest.

Authors' Declaration

The authors hereby declare that the work presented in this article is original and any liability for claims relating to the content will be borne by them.

Acknowledgements

The authors are grateful for the financial support from *Beasiswa Pendidikan Indonesia* (BPI)/Lembaga Pengelola Dana Pendidikan (LPDP), Ministry of Finance, Republic of Indonesia, with decree No. 0691/J5.2.3/BPI.06/10/2021.

References

1. Bray F, Laversanne M, Sung H, Ferlay J, Siegel RL, Soerjomataram I, Jemal A. Global cancer statistics 2022: GLOBOCAN estimates of incidence and mortality worldwide for 36 cancers in 185 countries. CA Cancer J Clin. 2024; 74(3): 229–263; doi: 10.3322/caac.21834.
2. American Cancer Society. Cancer Facts and Figures. 2020. Atlanta: American Cancer Society; 2020. 15 p.
3. Naik S, Larsen SB, Cowley CJ, Fuchs E. Two to tango: Dialog between immunity and stem cells in health and disease. Cell. 2018; 175(4): 908–920; doi: 10.1016/j.cell.2018.08.071.
4. Sati P, Sharma E, Dhyani P, Attri DC, Rana R, Kiyekbayeva L, Büsselberg D, Samuel SM, Sharifi-Rad J. Paclitaxel and its semi-synthetic derivatives: comprehensive insights into chemical structure, mechanisms of action, and anticancer properties. Eur J Med Res. 2024; 29(1): 90; doi: 10.1186/s40001-024-01657-2.
5. Rashmi M. A worldwide list of endophytic fungi with notes on ecology and diversity. Mycosphere. 2019; 10(1): 798–1079; doi: 10.5943/mycosphere/10/1/19.
6. Santos AL, Ionta M, Horvath R, Soares MG, de Medeiros LS, Uemi M, Kawafune ES, Tangerina MMP, Ferreira MJP, Sartorelli P. Molecular network for accessing polyketide derivatives from *Phomopsis* sp., an endophytic fungus of *Casearia arborea* (*Salicaceae*). Phytochem Lett. 2021; 42: 1–7; doi: 10.1016/j.phytol.2020.11.020.
7. Fathoni A, Ilyas M, Praptiwi, Wulansari D, Agusta A. Antibacterial and antioxidant activities of fungal endophytes isolated from medicinal plants in Simeulue Island, Aceh. Hayati. 2022; 29(6): 720–732; doi: 10.4308/hjb.29.6.720-732.
8. Abreu LM, Costa SS, Pfenning LH, Takahashi JA, Larsen TO, Andersen B. Chemical and molecular characterization of *Phomopsis* and cytospora-like endophytes from different host plants in Brazil. Fungal Biol. 2012; 116(2): 249–260; doi: 10.1016/j.funbio.2011.11.008.
9. Puig AS. Fungal pathogens of cacao in Puerto Rico. Plants. 2023; 12(22): 3855; doi: 10.3390/plants12223855.
10. Minarni, Artika IM, Julistiono H, Bermawie N, Riyanti EI, Hasim, Hasan AEZ. Anticancer activity test of ethyl acetate extract of endophytic fungi isolated from soursop leaf (*Annona muricata* L.). Asian Pac J Trop Med. 2017; 10(6): 566–571; doi: 10.1016/j.apjtm.2017.06.004.
11. Arifni F, Hasan A, Hasim, Julistiono H, Husnawaty, Bermawie N, Riyanti E. Anticancer activities of endophytic fungi isolated from soursop leaves (*Annona muricata* L.) against WiDr cancer cells. Annu Res Rev Biol. 2017; 18(5): 1–11; doi: 10.9734/ARRB/2017/34657.
12. Hasan AEZ, Julistiono H, Bermawie N, Riyanti EI, Arifni FR. Soursop leaves (*Annona muricata* L.) endophytic fungi anticancer activity against HeLa cells. Saudi J Biol Sci. 2022; 29(8): 103354; doi: 10.1016/j.sjbs.2022.103354.

13. Adeleke B, Babalola O. Pharmacological potential of fungal endophytes associated with medicinal plants: A review. J Fungi. 2021;7(2):147; doi: 10.3390/jof7020147.
14. Amirzakariya BZ, Shakeri A. Bioactive terpenoids derived from plant endophytic fungi: An updated review (2011–2020). Phytochemistry. 2022; 197: 113130; doi: 10.1016/j.phytochem.2022.113130.
15. Subban K, Kempken F. Insights into Taxol® biosynthesis by endophytic fungi. Appl Microbiol Biotechnol. 2023; 107(20): 6151–6162; doi: 10.1007/s00253-023-12713-y.
16. Lee C, Shim S-H. Endophytic fungi inhabiting medicinal plants and their bioactive secondary metabolites. Nat Prod Sci. 2020; 26(1): 10–27; doi: 10.20307/nps.2020.26.1.10.
17. Xu TC, Lu YH, Wang JF, Song ZQ, Hou YG, Liu SS, Liu CS, Wu SH. Bioactive secondary metabolites of the genus *Diaporthe* and anamorph *Phomopsis* from terrestrial and marine habitats and endophytes: 2010–2019. Microorganisms. 2021; 9(2): 217; doi: 10.3390/microorganisms9020217.
18. Irsal RAP, Gholam GM, Dwicesaria MA, Chairunisa F. Computational investigation of *Y. aloifolia variegate* as anti-Human Immunodeficiency Virus (HIV) targeting HIV-1 protease: A multiscale in-silico exploration. Pharmacol Res Mod Chin Med. 2024; 11: 100451; doi: 10.1016/j.prmcm.2024.100451.
19. Gholam GM, Mahendra FR, Irsal RAP, Dwicesaria MA, Ariefin M, Kristiadi M, Rizki AFM, Azmi WA, Artika IM, Siregar JE. Computational exploration of compounds in *Xylocarpus granatum* as a potential inhibitor of *Plasmodium berghei* using docking, molecular dynamics, and DFT studies. Biochem Biophys Res Commun. 2024; 733: 150684; doi: 10.1016/j.bbrc.2024.150684.
20. Gupta A, Meshram V, Gupta M, Goyal S, Qureshi KA, Jaremko M, Shukla KK. Fungal endophytes: Microfactories of novel bioactive compounds with therapeutic interventions; A comprehensive review on the biotechnological developments in the field of fungal endophytic biology over the last decade. Biomol. 2023; 13(7): 1038; doi: 10.3390/biom13071038.
21. Islam MA, Amin SMN, Brown CL, Juraimi AS, Uddin MK, Arshad A. Determination of median lethal concentration (LC_{50}) for endosulfan, heptachlor and dieldrin pesticides to African catfish, *Clarias gariepinus* and their impact on its behavioral patterns and histopathological responses. Toxics. 2021; 9(12): 340; doi: 10.3390/toxics9120340.
22. Alnuqaydan A, Almutary A, Azam M, Manandhar B, Yin G, Yen L, Madheswaran T, Paudel K, Hansbro P, Chellappan D, Dua K. Evaluation of the cytotoxic activity and anti-migratory effect of berberine–phytantriol liquid crystalline nanoparticle formulation on non-small-cell lung cancer in vitro. Pharmaceutics. 2022; 14(6): 1119; doi: 10.3390/pharmaceutics14061119.
23. Setiawati A. Anticancer activity of mangosteen pericarp dry extract against MCF-7 breast cancer cell line through estrogen receptor-α. Indones J Pharm. 2014; 25(3): 119; doi: 10.14499/indonesianjpharm25iss3pp119.
24. Balachandran P, Sathish Muthukrishnan, Balakrishnan SE. Inhibition of estrogen receptor alpha (Erα) by bioactive compounds from *Terminalia Arjuna* (Roxb. Ex Dc.) Wight & Arn.: A molecular docking study. J Microbiol Biotechnol Food Sci. 2024; 14(3): e11492; doi: 10.55251/jmbfs.11492.
25. Kawsar SMA, Hossain MA, Hosen MI, Parmar MP, Patel SG, Patel HM, Hasan I, Biswas S, Saleh MA. Novel benzylidene derivatives: Synthesis and their antimicrobial and anticancer studies and in silico investigations. Chem Phys Impact. 2025; 10:100786; doi: 10.1016/j.chphi.2024.100786.
26. Land H, Humble MS. YASARA: A tool to obtain structural guidance in biocatalytic investigations. Methods Mol Biol. 2018; 43–67; doi: 10.1007/978-1-4939-7366-8_4.
27. Patel A, Patel P, Sharma S. Anticancer activity, DFT calculation, ADMET study and molecular docking of synthetic chalcone (2E)-1-(4-aminophenyl)-3-(3,4,5-trimethoxyphenyl)-2-propen-1-one in breast cancer cell line (MCF-7). J Mol Struct. 2025; 1321: 140150; doi: 10.1016/j.molstruc.2024.140150.
28. Niran A. Al-Ogaili, Noor M. Mohammed. In silico study of the inhibitory effects of sanguinarine and its proposed derivative on phosphoinositide 3-kinase (PI3K) isoforms. Trop J Nat Prod Res. 2025; 9(10); doi: 10.26538/tjnpr/v9i10.29.
29. Eunice E, Prasana JC, Kadaikunnan S, Alharbi NS, Muthu S. Quantum mechanical, spectroscopic, docking studies (dementia & breast cancer) and *in-vitro* assays of phytochemical compound dehydrozingerone by DFT. J Mol Struct. 2025; 1319: 139354; doi: 10.1016/j.molstruc.2024.139354.
30. Ahmed SF, Barua P, Amin M Al, Tabassum R, Haque MME, Islam L, Hossain MS, Verma AK. Cheminformatics-based analysis identified novel compounds from *Nelumbo nucifera* as potential inhibitors targeting PI3k/Akt/mTOR Pathway of HR+/HER2- subtype for breast cancer. Biochem Biophys Res Commun. 2025; 791: 152953; doi: 10.1016/j.bbrc.2025.152953.
31. Hoque MdM, Jannati TE, Shourav MdAM, Rehman HM, Hammad HM, Haque J. N-Carbobenzoxy-L-Phenylalanine disrupts ErbB2 homodimer formation, blocking autophosphorylation and downstream signaling in breast cancer: A comprehensive computational approach. Comput Biol Med. 2025; 199: 111305; doi: 10.1016/j.compbiomed.2025.111305.
32. Ajanal MN, Sushma HN, Kottureshetty IB. Experimental brine shrimp (*Artemia Salina*) lethality assay to evaluate the drug incompatibility on combined administration of kakamachi (*Solanum nigrum*) and madhu (Honey). Indian Med J. 2021; 9(1): 28–32; doi: 10.4103/JISM.JISM_82_20.
33. Indriaty I, Ginting B, Hasballah K, Djufri. Assessment cytotoxic assay of *Rhizophora* plants mangrove using brine shrimp (*Artemia salina* L) model. IOP Conf Ser Earth Environ Sci. 2022; 951(1): 012070; doi: 10.1088/1755-1315/951/1/012070.
34. Nerdy N, Lestari P, Sinaga JP, Ginting S, Zebua NF, Mierza V, Bakri TK. Brine shrimp (*Artemia salina*) lethality test of ethanolic extract from green betel (*Piper betle* Linn.) and red betel (*Piper crocatum* Ruiz and Pav.) through the soxhletation method for cytotoxicity test. Open Access Maced J Med Sci. 2021; 9(A): 407–412; doi: 10.3889/oamjms.2021.6171.
35. Meyer B, Ferrigni N, Putnam J, Jacobsen L, Nichols D, McLaughlin J. Brine shrimp: A convenient general bioassay for active plant constituents. Planta Med. 1982; 45(05): 31–34; doi: 10.1055/s-2007-971236.
36. Aksono EB, Latifah AC, Suwanti LT, Haq KU, Pertiwi H. Clove flower extract (*Syzygium aromaticum*) has anticancer potential effect analyzed by molecular docking and brine shrimp lethality test (BSLT). Vet Med Int. 2022; 2022:1–7; doi: 10.1155/2022/5113742.
37. Handayani D, Artasasta MA, Safirna N, Ayuni DF, Tallei TE, Hertiani T. Fungal isolates from marine sponge *Chelonaplysilla* sp.: Diversity, antimicrobial and cytotoxic activities. Biodiversitas. 2020; 21(5); doi: 10.13057/biodiv/d210523.
38. Xu TC, Lu YH, Wang JF, Song ZQ, Hou YG, Liu SS, Liu CS, Wu SH. Bioactive secondary metabolites of the genus *Diaporthe* and anamorph *Phomopsis* from terrestrial and marine habitats and endophytes: 2010–2019. Microorganisms 2021; 9(2): 217; doi: 10.3390/microorganisms9020217.
39. Madar I, Sultan G, Chelliah R, Oh DH. Screening for anticancer activity: DNA fragmentation assay. In: Dharumadurai D (eds). Methods in Actinobacteriology.

Springer Protocols Handbooks. New York Humana; 2022; 439–442; doi: 10.1007/978-1-0716-1728-1_58.
40. Hariyanti H, Yanuar A, Kusmardi K, Hayun H. Synthesis and in vitro cytotoxic activity of novel indazole analogues of curcumin against MCF-7, HeLa, WiDr, and vero cell lines. J Appl Pharm Sci. 2022; 179–184; doi: 10.7324/JAPS.2022.120420.
41. Santos AL, Ionta M, Horvath RO, Soares MG, Silva DO, Kawafune ES, Ferreira MJP, Sartorelli P. Dereplication of cytochalasans and octaketides in cytotoxic extracts of endophytic fungi from *Casearia arborea* (Salicaceae). Metabolites. 2022; 12(10): 903; doi: 10.3390/metabo12100903.
42. Ahamed F, Murugan M. Isolation and characterization of marine endophytic fungi from seaweeds, and bioactivity of their crude extracts. J Pure Appl Microbiol. 2019; 13(3): 1451–1460; doi: 10.22207/JPAM.13.3.15.
43. Alam B, Li J, Ge Q, Khan MA, Gong J, Mehmood S, Yuán Y, Gong W. Endophytic fungi: from symbiosis to secondary metabolite communications or vice versa? Front Plant Sci. 2021; 12; doi: 10.3389/fpls.2021.791033.
44. Viedma-Rodríguez R, Baiza-Gutman L, Salamanca-Gómez F, Diaz-Zaragoza M, Martínez-Hernández G, Esparza-Garrido Rr, Velázquez-Flores Ma, Arenas-Aranda D. Mechanisms associated with resistance to tamoxifen in estrogen receptor-positive breast cancer (Review). Oncol Rep. 2014; 32(1): 3–15; doi: 10.3892/or.2014.3190.
45. Ali S, Rasool M, Chaoudhry H, Pushparaj PN, Jha P, Hafiz A, Mahfooz M, Sami GA, Kamal MA, Bashir S, Ali A, Jamal MS. Molecular mechanisms and mode of tamoxifen resistance in breast cancer. Bioinformation. 2016; 12(3): 135–139; doi: 10.6026/97320630012135.
46. Kari S, Subramanian K, Altomonte IA, Murugesan A, Yli-Harja O, Kandhavelu M. Programmed cell death detection methods: A systematic review and a categorical comparison. Apoptosis. 2022; 27(7–8): 482–508; doi: 10.1007/s10495-022-01735-y.
47. Bakadlag R, Limniatis G, Georges G, Georges E. The anti-estrogen receptor drug, tamoxifen, is selectively lethal to p-glycoprotein-expressing multidrug resistant tumor cells. BMC Cancer. 2023; 23(1): 24; doi: 10.1186/s12885-022-10474-x.
48. Shanle EK, Xu W. Selectively targeting estrogen receptors for cancer treatment. Adv Drug Deliv Rev. 2010; 62(13): 1265–1276; doi: 10.1016/j.addr.2010.08.001.
49. Ali S, Rasool M, Chaoudhry H, Pushparaj PN, Jha P, Hafiz A, Mahfooz M, Sami GA, Kamal MA, Bashir S, Ali A, Jamal MS. Molecular mechanisms and mode of tamoxifen resistance in breast cancer. Bioinformation. 2016; 12(3): 135–139; doi: 10.6026/97320630012135.
50. Hadisaputri YE, Habibah U, Abdullah FF, Halimah E, Mutakin M, Megantara S, Abdulah R, Diantini A. Antiproliferation activity and apoptotic mechanism of soursop (*Annona muricata* L.) leaves extract and fractions on MCF7 breast cancer cells. Breast Cancer. 2021; 13: 447–457; doi: 10.2147/BCTT.S317682.
51. Wang J, Xu Z, Hu X, Yang Y, Su J, Liu Y, Zhou L, Qin J, Zhang D, Yu H. Epoxycytochalasin H: An endophytic *Phomopsis* compound induces apoptosis in A2780 cells through mitochondrial damage and endoplasmic reticulum stress. Onco Targets Ther. 2020; 13: 4987–4997; doi: 10.2147/OTT.S253716.
52. Ahmed I, Hussain H, Schulz B, Draeger S, Padula D, Pescitelli G, van Ree T, Krohn K. Three new antimicrobial metabolites from the endophytic fungus *Phomopsis* sp. European J Org Chem. 2011; 2011(15): 2867–2873; doi: 10.1002/ejoc.201100158.
53. Beekman AM, Barrow RA. Syntheses of cytosporones A, C, J, K, and N, metabolites from medicinal fungi. Aust J Chem. 2015; 68(10): 1583; doi: 10.1071/CH15144.
54. Kim HH, Jeong SH, Ha SE, Park MY, Bhosale PB, Abusaliya A, Won CK, Heo JD, Kim HW, Kim GS. Cellular regulation of kynurenic acid-induced cell apoptosis pathways in AGS cells. Int J Mol Sci. 2022; 23(16): 8894; doi: 10.3390/ijms23168894.
55. Dibha A, Wahyuningsih S, Ansori A, Kharisma V, Widyananda M, Parikesit A, Sibero M, Probojati R, Murtadlo A, Trinugroho J, Sucipto T, Turista D, Rosadi I, Ullah M, Jakhmola V, Zainul R.. Utilization of secondary metabolites in algae *Kappaphycus alvarezii* as a breast cancer drug with a computational method. Pharmacogn J. 2022; 14(3): 536–543; doi: 10.5530/pj.2022.14.68.
56. Lei J, Wang Q, Li G, Li Y, Zhang P, Xu G. *β*-Caryophyllene from chilli pepper inhibits the proliferation of non-small cell lung cancer cells by affecting miR-659-3p-targeted sphingosine kinase 1 (SphK1). Int J Gen Med. 2021; 14: 9599–9613; doi: 10.2147/IJGM.S338513.
57. Noser AA, Shehadi IA, Abdelmonsef AH, Salem MM. Newly synthesized pyrazolinone chalcones as anticancer agents via inhibiting the PI3K/Akt/ERK1/2 signaling pathway. ACS Omega. 2022; 7(29): 25265–25277; doi: 10.1021/acsomega.2c02181.
58. Constantinescu T, Lungu CN. Anticancer activity of natural and synthetic chalcones. Int J Mol Sci. 2021; 22(21): 11306; doi: 10.3390/ijms222111306.
59. Huang Z, Cai X, Shao C, She Z, Xia X, Chen Y, Yang J, Zhou S, Lin Y. Chemistry and weak antimicrobial activities of phomopsins produced by mangrove endophytic fungus *Phomopsis* sp. ZSU-H76. Phytochemistry. 2008; 69(7): 1604–1608; doi: 10.1016/j.phytochem.2008.02.002.
60. Shabana SM, Gad NS, Othman AI, Mohamed AF, El-Missiry MA. *β*-caryophyllene oxide induces apoptosis and inhibits proliferation of A549 lung cancer cells. Med Oncol. 2023; 40(7): 189; doi: 10.1007/s12032-023-02022-9.
61. Kongprapan T, Xu X, Rukachaisirikul V, Phongpaichit S, Sakayaroj J, Chen J, Shen X. Cytosporone derivatives from the endophytic fungus *Phomopsis* sp. PSU-H188. Phytochem Lett. 2017; 22:219–223; doi: 10.1016/j.phytol.2017.10.002.
62. Jamshed L, Debnath A, Jamshed S, Wish J V., Raine JC, Tomy GT, Thomas PJ, Holloway AC. An emerging cross-species marker for organismal health: tryptophan-kynurenine pathway. Int J Mol Sci. 2022; 23(11): 6300; doi: 10.3390/ijms23116300.
63. Walczak K, Wnorowski A, Turski WA, Plech T. Kynurenic acid and cancer: facts and controversies. Cell Mol Life Sci. 2020; 77(8): 1531–1550; doi: 10.1007/s00018-019-03332-w.
64. Wu Y, Xu J, Liu Y, Zeng Y, Wu G. A review on anti-tumor mechanisms of coumarins. Front Oncol. 2020; 10; doi: 10.3389/fonc.2020.592853.
65. Rudrapal M, Khan J, Dukhyil AA Bin, Alarousy RMII, Attah EI, Sharma T, Khairnar SJ, Bendale AR. Chalcone scaffolds, bioprecursors of flavonoids: chemistry, bioactivities, and pharmacokinetics. Molecules. 2021; 26(23):7177; doi: 10.3390/molecules26237177.
66. Khan MF, Kader F Bin, Arman M, Ahmed S, Lyzu C, Sakib SA, Tanzil SM, Zim AFMIU, Imran MdAS, Venneri T, Romano B, Haque MdA, Capasso R. Pharmacological insights and prediction of lead bioactive isolates of Dita bark through experimental and computer-aided mechanism. Biomed Pharmacother. 2020; 131:110774; doi: 10.1016/j.biopha.2020.110774.
67. Milusheva M, Gledacheva V, Stefanova I, Pencheva M, Mihaylova R, Tumbarski Y, Nedialkov P, Cherneva E, Todorova M, Nikolova S. In silico, in vitro, and ex vivo

biological activity of some novel mebeverine precursors. Biomedicines. 2023; 11(2): 605; doi: 10.3390/biomedicines11020605.
68. Sehrawat R, Rathee P, Rathee P, Khatkar S, Akkol EK, Khatkar A, Sobarzo-Sánchez E. In silico design of novel bioactive molecules to treat breast cancer with chlorogenic acid derivatives: A computational and SAR approach. Front Pharmacol. 2023; 14; doi: 10.3389/fphar.2023.1266833.
69. Gao K, Wang R, Chen J, Cheng L, Frishcosy J, Huzumi Y, Qiu Y, Schluckbier T, Wei X, Wei GW. Methodology-centered review of molecular modeling, simulation, and prediction of SARS-CoV-2. Chem Rev. 2022; 122(13): 11287–11368; doi: 10.1021/acs.chemrev.1c00965.
70. Hussein K, Shihab N, Saeed B. Anti-cancer, anti-osteoporosis, and molecular docking studies of novel chalcone and epoxy chalcone. Biointerface Res Appl Chem. 2021; 12(5): 6668–6685; doi: 10.33263/BRIAC125.66686685.
71. Mohanasundaram S, Karthikeyan P, Sampath V, Anbazhagan M, Prabhu SV, Khaled JM, Thiruvengadam M. Molecular docking, dynamics simulations, ADMET, and DFT calculations: Combined in silico approach to screen natural inhibitors of 3CL and PL proteases of SARS-CoV-2. Cell Microbiol. 2024; 2024: 1–19; doi: 10.1155/2024/6647757.
72. Mahmud S, Biswas S, Paul GK, Mita MA, Afrose S, Hasan MR, Shimu MSS, Uddin MAR, Uddin MS, Zaman S, Kibria KMK, Khan MA, Emran TB, Saleh MA. Antiviral peptides against the main protease of SARS-CoV-2: A molecular docking and dynamics study. Arab J Chem. 2021; 14(9): 103315; doi: 10.1016/j.arabjc.2021.103315.
73. David CC, Jacobs DJ. Principal component analysis: A method for determining the essential dynamics of proteins. Methods Mol Biol. 2014; 1084: 193–226; doi: 10.1007/978-1-62703-658-0_11.
74. Skjærven L, Yao XQ, Scarabelli G, Grant BJ. Integrating protein structural dynamics and evolutionary analysis with Bio3D. BMC Bioinformatics. 2014; 15(1): 399; doi: 10.1186/s12859-014-0399-6.
75. Xu X, Wang J, Yan B, Leng Y, Chen Z, Pan G, Xiang C, Teng Y. Synthesis, in vitro cytotoxicity evaluation and mechanism of 5′ monosubstituted chalcone derivatives as antitumor agents. Bioorg Med Chem Lett. 2023; 85: 129239; doi: 10.1016/j.bmcl.2023.129239.
76. Deka D, Das SRC, Das T, Chakraborty P, Kar K, Chowdhury S. Chalcone derivatives: In silico design, molecular docking study and anticancer activity on MCF-7 cells. Silico Res Biomed. 2025; 1:100016; doi: 10.1016/j.insi.2025.100016.
77. Upadhyaya S, Shetty CR, Nayak UY, S SRK, Shetty S, Likhitha U. Thiophene functionalised chalcones with anticancer potential: Synthesis, molecular docking, molecular dynamics, and cytotoxicity evaluation. J Mol Struct. 2026; 1350: 144115; doi: 10.1016/j.molstruc.2025.144115.